RIGA TECHNICAL UNIVERSITY

Faculty of Mechanical Engineering, Transport and Aeronautics

Institute of Mechanical Engineering

Antons Štekleins

Doctoral Student of the Study Programme "Production Technology"

RESEARCH ON VACUUM GAUGE TESTING METHODOLOGY

Summary of the Doctoral Thesis

Scientific supervisor

Professor Dr. sc. ing.

ĒRIKS GERIŅŠ

RTU Press

Rīga 2018

Stekleins A. Research on Vacuum Gauge Testing Methodology. Summary of the Doctoral Thesis. – Riga: RTU Press, 2018. – 49 p.

Printed in accordance with the decision of the Promotion Council "RTU P-16" of 14 September 2017, Minutes No. 3.

ISBN 978-9934-22-065-4 (print)

ISBN 978-9934-22-066-1 (pdf)

DOCTORAL THESIS PROPOSED TO RIGA TECHNICAL UNIVERSITY FOR THE PROMOTION TO THE SCIENTIFIC DEGREE OF DOCTOR OF ENGINEERING SCIENCES

To be granted the scientific degree of Doctor of Engineering Sciences, the present Doctoral Thesis has been submitted for the defence at the open meeting of RTU Promotion Council on 17 April 2018 at the Faculty of Mechanical Engineering, Transport and Aeronautics of Riga Technical University, 36a Viskalu Street 36a, Room 405.

OFFICIAL REVIEWERS

Professor Dr. habil. sc. ing. Viktors Mironovs
Riga Technical University

Professor Dr. sc. ing. Ēriks Kronbergs
Latvia University of Agriculture

Professor Dr. habil. Sigitas Tamulevicius
Kaunas University of Technology, Lithuania

DECLARATION OF ACADEMIC INTEGRITY

I hereby declare that the Doctoral Thesis submitted for the review to Riga Technical University for the promotion to the scientific degree of Doctor of Engineering Sciences is my own. I confirm that this Doctoral Thesis had not been submitted to any other university for the promotion to a scientific degree.

Antons Stekleins ……. (signature)

Date: ……

The Doctoral Thesis has been written in Latvian. It consists of Introduction; 6 Chapters; Conclusion; 69 figures; 38 tables; 2 appendices; the total number of pages is 106. The Bibliography contains 74 titles.

CONTENT

GENERAL DESCRIPION OF DOCTORAL THESIS

TOPICALITY

Nanotechnology has progressed rapidly as a science in last few years and has been adopted by many industries: medicine, mechanical industry, aviation and other significant industries. Very common and in demand are optically transparent covers that are used in construction. Modern electronic circuits utilize thin transparent conductive layers of nanomaterials. Thanks to their unique properties, these materials are most frequently used in touch sensitive screen manufacturing. Each nanolayer has its own design characteristics, for example the goal of the design of optically transparent nanolayers is layer thickness and transparency factor.

In case of optically transparent materials nanolayer integration with other materials is carried through magnetic strain in vacuum chamber on a sheet type or roll type materials such as fabric, metal foil and film. Properties of such nanomaterial are determined by technological values that are used in this process, such as pressure and environment in vacuum chamber. During the beginning of technological process, and precisely in straining process, it is extremely important to use a reliable vacuum gauge that measures pressure inside the vacuum chamber. Pressure changes vibration, and pollution negatively affects the produced nanolayer properties and visual look. Precision and replicability of vacuum gauge during production in such way can decrease, thus making stable production significantly harder. In case of imprecise pressure measurement, sensor must be carefully taken to the nearest accredited test laboratory for calibration according to the required standards and regulations. There is no documented timeframe for calibrated vacuum gauge to sustain its precision, it is dependent on environment that is being used and other factors. It means that there is a period of time during when vacuum gauge results are starting to drift away, thus the absolute value of measured pressure error is increasing and affecting the technological process. This can be a serious problem if no calibration and recalibration policy has been established. Without regular checking of vacuum gauge and thorough inspection of the acquired data, the specific measurement device cannot be trusted, and it is not possible to strain nanolayer with required properties.

RESEARCH PROBLEM

Vacuum gauge operations are being researched in this doctoral thesis. Error of pressure measurements and the resulting negative implications on visual status and overall properties of the nanolayer is the most significant problem in vacuum chamber magnetic strain technology. To achieve better research results and to shorten the time period needed for vacuum gauge testing, a new vacuum gauge testing device has been engineered and produced, which supports 2×10^{-6} Torr pressure range in approximate period of 20 minutes. Multi-functional tests had been done using laboratory vacuum device UV80 and a newly produced experimental device

in order to research the precision of devices, result replicability, and to check ionization vacuum gauge correction function and gas delivery system elements. Based on vacuum gauge research results, a new vacuum gauge test methodology was developed for nanocover deposition process that allows to test vacuum gauges with different methods, as well as other vacuum gauge parts that affect technological process. Such methods are: design and implementation and maintenance of measurement result data base; development of vacuum pressure measurement behavioural model; implementation of the desired correction factor in case of vacuum gauge permanent error, thus sustaining technological process and lowering the device downtime in order to meet technological demands for nanolayer.

AIM AND OBJECTIVES OF THE RESEARCH

The aim of the doctoral thesis is to research and develop vacuum gauge testing methodology.

The following objectives had been defined to reach the aim.

1) To analyze principal operations, construction, advantages and disadvantages of different vacuum gauges and their usage depending on their pressure range, environment and nanolayer deposition process.
2) To engineer and produce experimental vacuum gauge test device that ensures pressure range limits of 2×10^{-6} Torr.
3) To research ionization and diaphragm vacuum gauge operation using multifunctional experimental methods, thus obtaining the data about vacuum gauge operation and pressure measurement error.
4) To perform a SiO_2 nanolayer deposition process and research dependency of pressure on nanolayer visual condition and properties.
5) To develop fuzzy logic models for the prediction of thickness and transparency of a SiO_2 nanolayer in flow/drain conditions.

RESEARCH METHODS AND TOOLS

The doctoral thesis presents the research that has been done using a newly produced experimental testing device as well as the device UV80. The following devices were used during the research: ionization vacuum gauge HPG 400 and BPG 402, and diaphragm vacuum gauge CDG 025D.

Experimental results were presented using Microsoft Excel and Microsoft Word software. Sucking mathematical simulation of the produced vacuum gauge testing equipment was done using OCTAVE software.

For testing purposes of silicon dioxide (SiO_2) nanolayer properties the following devices were used: for nanolayer thickness – spectroscopic reflectometer FILMETRICS F20-UV ("Sidrabe", Inc.), for transparency factor – MC 122 spectrophotometer ("Sidrabe", Inc.).

Based on experimental research and the obtained results, a fuzzy logic model was developed for nanolayer thickness and transparency factor. For these fuzzy logic models and for the presentation of their results a specific software (FuzzyTECH) was used.

Using laboratory vacuum device UV80, a research on pressure oscillation effect on silicon dioxide nanolayer was conducted focused on thickness and transparency. The technological process of nanolayer deposition was done at different pressures, and the results were used to develop nanolayer sample reflection models.

SCIENTIFIC INNOVATION

1) For the first time a fuzzy logic was used in SiO_2 nanolayer thickness and transparency factor prediction by imitating drain condition during the technological process.
2) New experimental vacuum gauge testing device has been produced that allows to conduct multifunctional research based on which a new test methodology was developed.
3) Full pressure measurement is allowing to evaluate parameters of technological process.

THESIS STATEMENTS TO BE DEFENDED

1) Vacuum gauge testing methodology.
2) New experimental vacuum gauge testing device.
3) Fuzzy logic model for SiO_2 nanolayer transparency factor and thickness prediction by imitating drain condition during technological process.

PRACTICAL APPLICATION

The newly developed vacuum gauge testing methodology ensures precise and thorough testing of vacuum gauge and other vacuum system elements, using a specifically newly developed and produced experimental device in order to ensure technological process, visual status and properties.

By using the described methods it is possible to make a data base of the particular vacuum gauge pressure behaviour and a model, which can be changed and adopted depending on the experimental method. Whereas newly engineered and produced vacuum test device allows to conduct vacuum gauge test quickly and effectively thanks to construction solutions and turbo molecular pump.

Using this methodology, vacuum gauge calibration time can be determined based on experimental testing results. To ensure the technological process of nanolayer deposition, it is crucial to use a precise reference vacuum gauge and in case of a problem try to solve any mismatch as soon as possible. The methodology can be used as a handbook to test vacuum gauges.

The developed fuzzy logic models for SiO_2 nanolayer property prediction imitate logical thinking process and present the effect of the selected parameters on nanolayer properties. Thanks to fuzzy logic models it is possible to determine the resources needed for favourable nanolayer properties, thus shortening the time and resources in case of non-efficient nanolayer production.

1. VACUUM TECHNOLOGY

1.1. Vacuum, basic principles and application

Nowadays nanotechnology is developing and is used in many industries, especially in mechanical engineering. It is a known fact that nanoparticles that are being produced with the help of nanotechnological process are being used in mechanical engineering, construction and electronics. To produce unique materials with different strain methods in vacuum and conduct specific experiments for further research, vacuum devices or vacuum system is needed that ensures and produces a favourable environment for realization of the technological process. Vacuum, which is the basis of this system, can be defined as gas pressure, which when filling a limited volume of container is lower than atmospheric pressure.

In mechanical engineering nanotechnology can be used in coating of cutting instruments, thus improving multiple parameters. It improves durability, increases hardness and sustainability ensuring higher speed of production and lower friction factor. The most widely used instrument coatings are TiN, and TiAlN. Nanolayers are used not only for mechanical instruments but also on any other elements of devices that demand higher mechanical properties. Using nanotechonolgy it is possible to strain nanolayers of various materials, such as aluminum or titan, if needed.

Vacuum technological process is not entirely researched, and one of significant factors that needs a deeper investigation is process control, replicability and stability, as well as the correlation of measuring instrument accuracy and the nanolayer. The main part of vacuum technological process is vacuum or pressure. Pressure can be described as ratio of evenly distributed perpendicular force applied to a flat area unit [21]

$$P = \frac{F}{A}, \tag{1.1}$$

where P is pressure (Pa); F is force (N); and A is area (m^2).

Smearing TiO ceramics with magnetoceramic straining technological process demands inert gas (argon) or oxygen. Gas mixture consists of multiple gas components that inherit corresponding pressure that is defined as partial pressure [21].

Overall gas partial pressure is described by gas laws. Partial pressure is defined by Dalton law: total gas mixture pressure is equal to the sum of partial pressure of mixture components and can be expressed as [40]

$$P = \sum_{i=1}^{k} p_i. \tag{1.2}$$

The equation for gas pressure determination supports three main gas parameters: molecular concentration, pressure and temperature, and is expressed with [40]

$$P = nkT, \tag{1.3}$$

where n is concentration of gas molecules; k is Boltzmann constant $(1{,}38 \times 10^{-23}, \frac{\mathrm{J}}{\mathrm{K}})$ [21]; and T is temperature.

Ideal gas equation can be expressed as [40]

$$P = \frac{Nm}{VM} RT, \tag{1.4}$$

where M is molar mass of gas; V is volume of gas; R is universal gas constant $R = 8{,}31 \times 10^3 \ \frac{\text{J}}{\text{K·mol}}$ [40]; and N is Avogadro number.

Pressure in SI system is measured in Pascal (Pa), gas flow is measured as cubic meter per second ($\frac{\text{m}^3}{\text{s}}$), whereas in vacuum technology industry pressure is measured in Torr, and gas flow – in standard cubic millimeters per minute (sccm).

1.2. Design of vacuum system

Vacuum system by its design elements can be different depending on the technical demands or product that we want to produce. Common and most widely used nanolayer carrier way is a magnetronic smearing on polymer film, metal foil and glass. Vacuum monolayers improve material and instrument properties. For example, using TiN nanolayer for cutting instruments improves their firmness, durability and total service time [18], [11], [23], [28].

Figure 1.1. depicts a vacuum device with magnetronic smearing that is designed for smearing covers of silver and silver oxide on variety of material foundations.

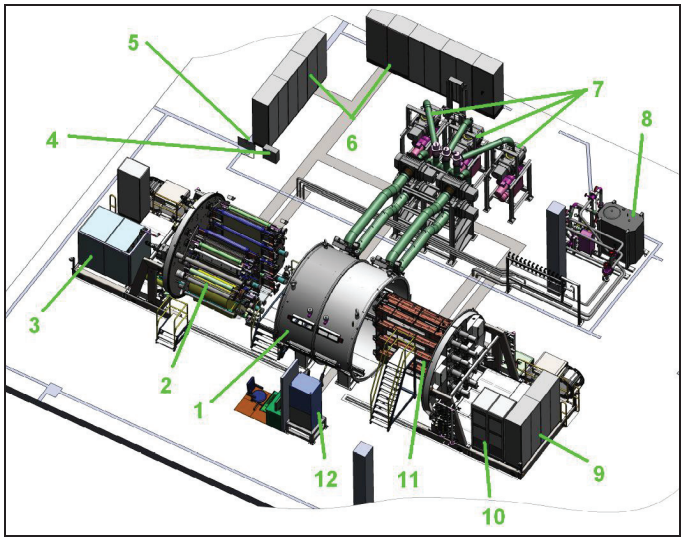

Fig. 1.1. Example of vacuum system.

Elements of vacuum system:

1) vacuum chamber;
2) rewinding system;
3) termostating system (roll cooling and heating);
4) gas input and distribution shelf;

5) compressed air input and distribution block;
6) electrical control shelf (processors, frequency converters, power supplies);
7) vacuum pump;
8) distilled water station (for magnetron and screen cooling);
9) electrical control shelf;
10) magnetron power supply;
11) magnetron;
12) cryopump (H_2O stream freezing)

The vacuum chamber should be hermetic and preferably made of stainless steel, which ensures that gas excitation from material surface is lower, thus achieving better degree of vacuum. Vacuum chamber pumping can be achieved with different pumps. Knowing chamber data, such as dimensions and volume before the pump is chosen, a model of pumping system and calculation of pumping velocity must be considered in order to know how fast and with what pressure this can be achieved, thus gaining information about the type of pump to be used. In many cases precise optical spray system works with a magnetron of a round form [32]. To achieve fast sedimentation, in most cases a reactive impulse magnetron spray is used [32].

Gas flow system is an important vacuum system element that is designed for nanolayer smearing technological process. Gas system usually consists of gas chambers, gas flow measurement devices (MFC Mass Flow Controller) and connections. MFSs are designed to regulate the amount of gas flow that is fed into the vacuum chamber.

Vacuum systems contain a glow discharge element that is responsible for cleaning the surface before the smearing process. Film cleaning before the beginning of the process is significant because it is the major factor in adhesion [47]. Before nanolayer smearing in vacuum chamber, the surface area is cleaned with ions [47]. Ion processing is good for upper layer removal where most of defects are located, it also activates the upper layer surface through radiation defects and chemical bond disruption [47]. Ion processing is done by glow discharge plasma or negative offset –100 V [47]. Basic processing uses glow discharge plasma under the pressure of 5×10^{-2} Torr $- 5 \times 10^{-1}$ Torr, therefore the pumping is done with a pre-vacuum pump. In addition to that, gas input is done: argon, oxigen or mixture of both. Glow discharge design uses two planes on which voltage is applied [47].

In most cases two vacuum gauges are used; one of them is measuring medium and low vacuum pressure and is considered to be a more precise measurement device and a reference device during the nanolayer deposition process. The other vacuum gauge is used for measuring high vacuum pressure. The basic principle of vacuum gauge is related to vacuum system pressure, therefore before choosing vacuum gauge it has to be considered in what conditions, temperature, pollution, and pressure it will operate. All vacuum gauges must be calibrated.

1.3. Methods of measuring pressure, and instrument classification

Vacuum gauges can be sorted by their type – direct or indirect. Direct devices are used in mechanical vacuum gauges, which operate on the principle that the pressure affects the elastic

element and as a result the element is deforming and this deformation is the criterion of the pressure. These direct principle devices are not dependent on gas.

Vacuum gauges with indirect operational principle are used to measure the dependence of different technological processes on pressure [40]. It means that these devices are measuring such parameters as thermal conductivity, ionization or viscosity that is dependent on molecular density [29]. This kind of vacuum gauges is dependent on gas and need to be calibrated for particular gas by using a reference etalon device.

Vacuum gauges can be classified by range of their pressure, although this is directly related to the principles of their operation. Thus, it is easier to determine whether the chosen device is compliant with application demands and can perform a precise and correct pressure measurement for technological process operation.

Company "Sidrabe", Inc. uses nanolayer magnetronic sputtering and two vacuum gauges in that process: hot cathode ionization vacuum gauge and diaphragm type vacuum gauge.

Vacuum gauges for low vacuum

For low vacuum pressure measurements, it is common practice to use diaphragm vacuum gauges. It is related to the fact that the elastic element is deforming, and its deformation is pressure factor. Elastic elements of deformation type devices can be membranes as well as tubes or other similar elements with similar material properties. It is assumed that vacuum gauges that measure pressure as force, are more reliable and more precise.

Most common operation of diaphragm devices is when the moving side of diaphragm is an electrode of plate capacitor and the other electrode (plate) is fixed, thus the bending diaphragm is changing the distance of two electrodes and the capacity of equivalent capacitor [5], [30], [8].

This diaphragm electrode usually is made of ceramics, and stainless steel; different materials result in different sensitivity [5], [21]. Using the ceramic diaphragm is one of the best possible solutions when vacuum is measured in aggressive environment such as aggressive gases [21]. Both ceramic and stainless steel devices have a design similar to the one shown in Fig. 1.2 [30].

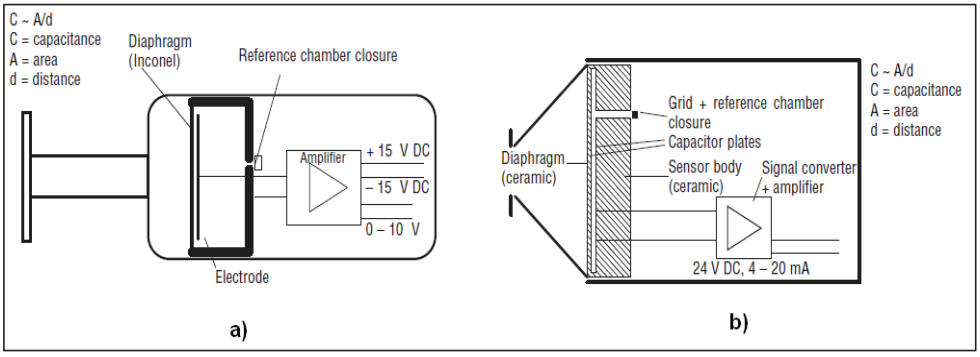

Fig. 1.2. Construction of diaphragm vacuum gauge using different diaphragms:
a – vacuum gauge with Inconel diaphragm; b – vacuum gauge with ceramic diaphragm.

Thickness of a diaphragm can be different because, working with different pressures, mean force that is applied on diaphragm may differ and the device operation is requiring optimal elastic properties, thus providing reliable results [30].

If (d) is evenly loaded diaphragm deformation, then pressure that is read from vacuum gauge can be expressed as [1]

$$P = \frac{dEt^3}{kr^4}, \tag{1.5}$$

where P is diaphragm pressure; E is diaphragm material elastic constant; r, t are diaphragm diameter and thickness; and k is constant.

This equation describes the nature of linear proportion of diaphragm deformation and pressure [1]. The devices that utilize diaphragm concept have very high precision, but possible range of measurable pressure is dependent on the mechanical properties of a particular diaphragm.

Vacuum gauges for medium vacuum

Pressure measurements of medium vacuum use different approach than the mechanical measurements because molecular density is too low for mechanical force to take action [1]. Common practice in this range is to measure the thermal conductivity of gas. Thermal conductivity is defined as the amount of thermal carriage that flows through plane surface area perpendicular to flow direction per time unit, and is divided by temperature gradient [1]. In other words, when molecules reach the heated glower, heat is emitted into gas, also thermal conductivity and thermal carriage velocity is dependent on thermal conductivity of gas [29]. Thermal conductivity of substrate can be expressed as [19]

$$H = -K\left(\frac{dT}{ds}\right), \tag{1.6}$$

where H is thermal amount that flows through an area unit per time unit in the direction that is parallel to (s); and $\frac{dT}{ds}$ is temperature gradient [19].

Derivation of thermal conductivity expression leads to the conclusion that thermal conductivity of thinned gas is the following [19]:

$$K = \frac{1}{4}(9y - 5)\eta C_v, \tag{1.7}$$

where y $= \frac{C_p}{C_v}$ – is difference between specific gas heat at constant pressure and constant volume; and n is viscosity factor [19].

Pirani vacuum gauge is the one that uses the property of gas thermal conductivity and thus is classified as thermal vacuum gauge [10]. Pirani vacuum gauge uses gas thermal conductivity at pressure that is lower than approximately 10–100 hPa [21]. This vacuum gauge is measuring pressure based on glower resistance measurement, thus leading to glower temperature [1].

$$R_T = R_0(1 + \alpha T), \tag{1.8}$$

where R_T is glower resistance at temperature $\mathrm{T}^0\mathrm{C}$ [1]**;** R_0 is resistance at $0\,^\circ\mathrm{C}$ [1]; and α – is glower resistance temperature factor [1].

Pirani vacuum gauge glower thickness is in the range of 5─20 μm in diameter [29]. The following materials can be used for making glower: nickel, iridium, platinum, or tungsten [29], [35]. Pirani vacuum gauge has limitations [21].

1) Pressure has little impact on thermal conductivity in the range of 10 hPa until normal atmosphere pressure (this is dependent on the type of gas) [21].
2) Thermal conductivity of gas is small compared to thermal carriage on glower ends at pressure lower than 10^{-4} hPa, thus not affecting glower thermal return [21].

Pirani vacuum gauge is sensitive to different types of gases in vacuum system because gases with different mass have different thermal volume and glower surface [4]. The results of vacuum gauge can contain error if it is calibrated for dry air and is actually used to measure argon [4].

Thermocouple vacuum gauge uses the property of thermal conductivity of gas where glower is being heated with a constant energy source [6]. In thermocouple vacuum gauge glower (Fig. 1.3. *1*), temperature is measured with thermocouple (Fig. 1.3. *2*), and electrodes are placed in glass or metallic casing (Fig. 1.3. *3*) that is connected with vacuum system [12], [40]. An example of such thermocouple is shown in Fig. 1.3 [47].

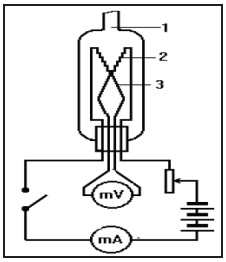

Fig. 1.3. Principal electric circuit of thermocouple vacuum gauge ПМТ-2:
1 – casing; 2 – glower; 3 – thermocouple.

For measuring electromotive force of thermocouple, a sensitive precise millivoltmeter is used, on the other hand, current is being measured with mili ammeter [40]. Thermocouple vacuum gauges like Pirani vacuum gauges use the property of constant current flowing in glower or glower's temperature.

Figure 1.4. shows pressure dependence of thermocouple vacuum gauge ПМТ-2 on the thermocouple electromotive force; the lower the pressure the lower is thermal conductivity and the temperature of heater rises [47].

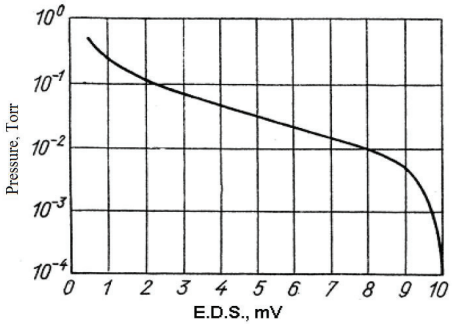

Fig. 1.4. Pressure dependence of ПМТ-2 on electromotive force in vacuum gauge.

The upsides of thermocouple converter are the following:

1) it measures overall pressure of all gases and fumes that are in vacuum system [40];
2) it supports constant measurement of pressure difference [40].

Vacuum gauges for measuring high vacuum

It is not possible to measure high vacuum with mechanical and thermal conductivity vacuum gauges because the molecular density is not sufficiently high. This is why for measurement of high vacuum pressure the devices with gas ionization property are used. The principle of operation of these vacuum gauges is based on direct proportionality of ion current and pressure created as a result of ionization of termoelectrons and remaining gas [47].

There are two types of ionization vacuum gauges: cold (Pening vacuum gauge) and hot cathode ionization vacuum gauges [34].

Cold cathode vacuum gauge. Cold cathode vacuum gauge consists of two electrodes: anode and cathode that have high voltage applied to them [21]. The principles of operation in cold cathode ionization vacuum gauge are as follows: negatively charged electrons move at high velocity through emission field traveling from cathode to anode [33], [21]. This electron flow ionizes neutral gas molecules that stimulate gas discharge [21]. The current resulting from this gas discharge that is measured, is the parameter that shows pressure [21].

Hot cathode vacuum gauge. Hot cathode vacuum gauge utilizes hot glower to emit electrons through thermoelectron emission [4], [21]. In other words, electrons are emitted with the help of hot cathode [4], [21]. This type of vacuum gauges consist of three main parts: anode, cathode and collector (Fig. 1.5.).

Principles of operation of hot cathode vacuum gauge are as follows: emitted electrons move through the anode grid that is open, and thus part of the electron flow travels through this grid and for a moment oscillates between the two sides of the grid until it comes in contact with the grid itself. [4], [17]. The developed ions are collected with the third electrode resulting in total current to be measured, thus the current and electron emission is related to pressure [4], [17].

In earlier times, Tungsten was the main material for cathodes, nowadays cathodes are made mainly of iridium and oxide nanolayers (Th_2O_3, Y_2O_3) to achieve higher stability against oxygen [30].

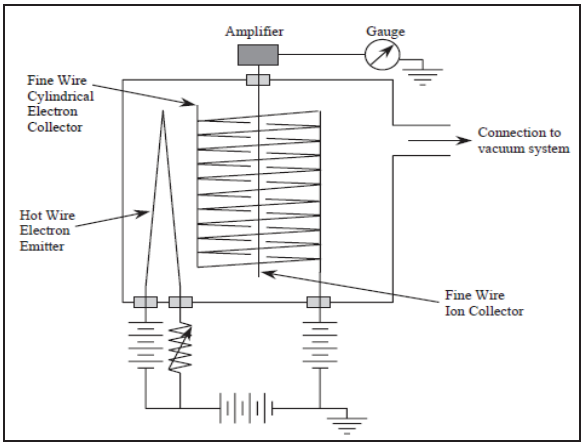

Fig. 1.5. Schematic diagram of hot cathode ionization vacuum gauge.

Generated current is directly related to gas density and thus to gas pressure [30].

1.4. Needs analysis for vacuum gauge precision, replicability and calibration

To ensure successful technological process and the resulting nanolayer, the vacuum gauge must be precise. Precision affects a number of aspects of the technological process; depending on the precision the amount of gas needed for the process may differ, as well as structure and visual properties (thickness, transparency factor) of the obtained nanolayer.

Each vacuum gauge has its own degree of precision, yet their principles of operation remain the same. For example, let us review the precision diagram of a rotation vacuum gauge of company VISOVAC (Fig. 1.6.) [1]. The precision of vacuum gauge is changing because of the changing pressure reaching the upper limit and lower limit of precision. This paradigm is applicable to all pressure measurement devices [1]. The precision of rotation vacuum gauges can increase or decrease depending on pressure and other factors, e.g. temperature [9], [31].

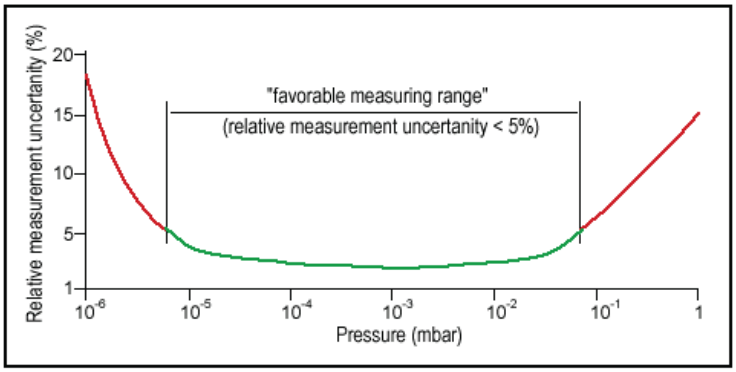

Fig. 1.6. VISCOVAC vacuum gauge measurement error dependency on pressure.

The reliable measurement area is marked in green and indicates that error is less than 5 %, which is usually called a high reliability region or suggested area of pressure measurements for particular device to be taken into account for successful nanolayer deposition onto the surface. Anything outside this region constitutes an error higher than 5 % and, moving away from the recommended region, shows measurement error rising significantly. This shows that care must be taken when choosing a proper device with properties that satisfy the quality demands of technological process.

If there is a high possibility that measurements will take place in environment with vibration, high temperature or pollution, which can give rise to a substantial the measurement error [1]. Vibration increases the measurement error [1].

The main quality parameters of a vacuum gauge are precision and result replicability; to achieve it the device needs to be calibrated periodically, in most cases it should be done annually (it must be taken into account that it is very hard to predict the recalibration period) [7], [29]. It is related to the fact that there are no developed standards and exploitation rules, thus every device operates under different environment, intensity, pollution, vibration and other factors. This is the main reason why each vacuum gauge must be calibrated depending on its operation and work load intensity. Data base of experimental measurements should be established for each device. Based on experimental measurements and on their comparison in different intervals, it is possible to obtain the model of vacuum gauge operation, to compare changes and produce always changing and renewing pressure model.

1.5. Calculation of vacuum gauge precision

Every measurement device has its own total measurement error that is a sum of all partial errors including systematic and random errors that are affecting the mechanics of the device [20]. When talking about vacuum gauge or measurement device precision, one must look for the device measurement error. Calibration and measurement accreditation usually is done by accredited laboratories where the device is tested, compared and calibrated with high grade etalon device [29]. Probability method [42], [50] has been chosen based on the following reference sources: The United Kingdom Accreditation Service and international office recommendation for calculating measurement uncertainty (UKAS); Bureau International des poids et mesures (BIPM).

The devices that are reviewed in the Thesis, such as ionization HPG 400, BPG 402 and diaphragm type CDG 025D vacuum gauges, were chosen for precision calculation. Every measurement sample has been taken 5 times. In total, 10 samples have been taken in different pressure ranges.

In experiments of pressure measurements, a diaphragm type device was set as reference result device because of its precision, thus ionization vacuum gauges were compared to these results. The results are shown in Table 1.1.

Table 1.1.

Vacuum Gauge Mean, and Mean Square Error Values

No.	CDG 025D		HPG 400 (SN547)		HPG 400 (SN 566)		BPG 402	
	x_{mean}, Torr	s_x, Torr	x_{mean}, Torr	s_x, Torr	x_{mean}, Torr	s_x, Torr	x_{mean}, Torr	s_x, Torr
1	1.23E-02	0.00022	4.71E-03	0.000012	1.14E-02	0.00043	1.15E-02	0.00042
2	9.73E-03	0.00003	3.47E-03	0.000028	9.78E-03	0.000026	9.74E-03	0.000032
3	8.61E-03	0.000025	2.95E-03	0.000070	8.79E-03	0.000017	8.5E-03	0.000039
4	7.35E-03	0.000037	2.28E-03	0.000039	7.42E-03	0.000017	7.1E-03	0.00003
5	6.73E-03	0.000021	2.02E-03	0.000025	6.6E-03	0.00007	6.42E-03	0.000015
6	5.52E-03	0.000012	1.44E-03	0.000033	5.63E-03	0.000027	4.75E-03	0.000019
7	4.33E-03	0.000019	1.20E-03	0.000014	4.29E-03	0.000018	3.24E-03	0.000021
8	3.70E-03	0.000013	2.44E-03	0.000028	3.73E-03	0.000015	3.00E-03	0.000014
9	2.41E-03	0.000016	1.38E-03	0.00003	2.41E-03	0.000016	1.35E-03	0.000015
10	1.67E-03	0.000011	2.1E-03	0.000033	1.67E-03	0.000011	1.22E-03	0.000071

When calculating a random error where credibility interval value is assumed 0.95 and measurement count is equal to 10, $t_\beta(N) = 2.23$. Random error is calculated as mean value from nine samples. For example, CDG 025D random error is calculated as follows:

$$\Delta x_s = \Delta x_{s_{mean}} = \frac{\sum s_x}{N} t_\beta(N) = \frac{0{,}000183}{9} \times 2.23 = 0.00005 \text{ Torr}. \quad (1.9)$$

Systematic error is determined separately for each device taking into account that diaphragm and ionization vacuum gauge errors are 0.2 % and ± 15 % [44], [45], [46].

$$\Delta x_\delta = \Delta x_{\delta_{mean}} = \frac{\sum \delta_{0,2\%}}{N} \times \frac{1}{3} t_\beta(\infty) = \frac{0{,}000098}{9} \times \frac{1}{3} \times 2.18 = 0.00001 \text{ Torr}. \quad (1.20)$$

To characterize the precision of measurements, relative error (ε) is used that is expressed as percentage and is calculated as follows [49]:

$$\varepsilon = \frac{\Delta x}{x_{vid}} 100\ \%. \quad (1.10)$$

The value of relative error always must be less than 100 %. If it is lower, it shows that measurements have been taken more precisely [49].

Relative error for CDG 025D has been calculated as an example in the following way:

$$\varepsilon = \varepsilon_{mean} = \frac{\sum \frac{\Delta x}{x_{mean}} 100\ \%}{N} = \frac{10.98}{9} = 1.22\ \%. \quad (1.11)$$

When calculating the relative error, random error is assumed as final error for the diaphragm vacuum gauge, whereas for all three ionization vacuum gauges systematic error is assumed as final error. Based on precise calculation we can conclude that there is a relative or total measurement error of 1.22 % for diaphragm vacuum gauge. Lower relative error indicates more precise measurement samples. Diaphragm vacuum gauge can be used as a reference measurement device in daily and experimental process even if it exceeds 0.2 % of the allowed error.

Literature review gives insight into vacuum and its basics, basic operation and construction of a vacuum system, as well as nanocoating application process. Review and analysis has been done on methods of pressure detection and measurement, vacuum gauge principles of operation, categories, precision, replicability, advantages and disadvantages. This allows to conclude that diaphragm vacuum gauge is considered to be amongst the best because

of its precision (0.2−05 % of measurement) and the fact that the results are not dependent on gas. In turn, ionization vacuum gauges operate on a different principle and their precision is substantially lower, just ±15% of measurements. In case of growing error, calibration process should take place. Calibration period is not standardized because of different operation environment and workload of a particular device. Calibration usually is offered as a final phase, but there are no alternative methods for vacuum gauge validation and adjustment. Company "Sidrabe", Inc. often uses diaphragm and ionization type vacuum gauges for vacuum processes, therefore based on the research problem and literature review the following goals have been set.

1) To choose two types of vacuum gauges − diaphragm and ionization − for experimental research based on literature review.
2) To engineer and produce experimental vacuum gauge testing device that satisfies the limited range of pressure of 2×10^{-6} Torr.
3) To research ionization and diaphragm vacuum gauge operation using multifunctional experimental methods thus gaining results about vacuum gauge operation and pressure measurement error.
4) To process silicon dioxide (SiO_2) nanolayer fetch-on technological process and research pressure factor on nanolayer visual status and properties.
5) To develop fuzzy logic model for SiO_2 nanolayer thickness and transparency factor prediction in sink conditions.

2. PRODUCTION OF NEW EXPERIMENTAL VACUUM DEVICE FOR VACUUM GAUGE TESTING

2.1. Production of new experimental vacuum device for multifunctional vacuum gauge testing

Vacuum gauge testing device is needed to test and verify vacuum gauge operation, precision, replicability as well as initial set of parameters of the vacuum gauge. The main task of experimental vacuum device is to ensure stable and satisfying vacuum for vacuum gauge testing and parameter setting. One of the jobs is to hold stable pressure and constant sucking speed in order to ensure that the tested vacuum gauges get the same pressure. When working with vacuum device and doing tests, a comparison method is used where one of the devices is compared with another with guaranteed high-level precision [14].

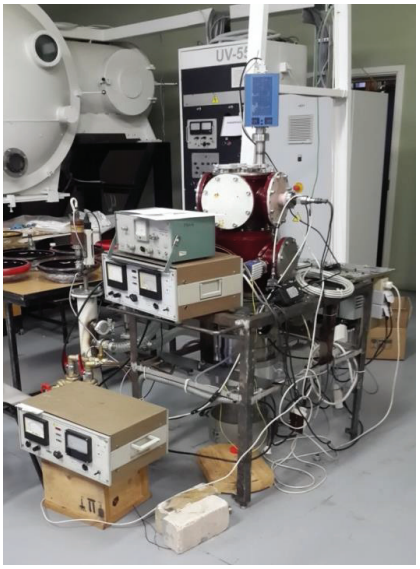

Fig. 2.1. Experimental vacuum gauge testing device.

Vacuum device consists of a metallic frame, steel chamber, automatically and manually regulated gate, turbomolecular pump TURBO-V3K-T, mechanical pump НВЗ-100Д, device control panel, vacuum gauge controller, pumping system tubes and valves, gas delivery system, and gas flow controller and regulation valve.

It is possible to test four devices simultaneously. The produced vacuum device shown in Fig. 2.1., allows reaching the border pressure of 2×10^{-6} Torr in a very short time period (~20 min).

2.2. Preparation of new experimental vacuum testing device for experiments

After the production and assembly of the vacuum device, it was tested for any sinks and for device border pressure, and was degassed.

While under the test, multiple sinks showed at welded seams that were resolved. The next step was the degassing operation. To speed this process up and to ensure maximal benefit of cleaning, the chamber was heated with a heater, thus higher vacuum level was achieved.

Before cleaning, vacuum chamber border pressure was 3×10^{-6} Torr, and after a long working and heating process the border pressure value of 8×10^{-7} Torr was achieved.

2.3. Modelling of pumping of experimental testing vacuum device using OCTAVE software

One of the main performance characteristic properties for vacuum nanolayer devices is the time during which the chamber gets pumped until the base pressure is reached [36]. Depending on the technological process, the pressure value can differ, but typically it is 1×10^{-5} mbar in process partition. If this value is reached, the partial pressure in gas chamber during process does not affect the process quality.

- Volume of vacuum chamber is V_1 (20 litre).
- Vacuum in separation V_1 is achieved using mechanical pump НВЗ-100Д and turbo molecular pump TURBO –V3K–T.

To find out how long it takes to produce the base pressure, the problem can be expressed as a differential equation:

$$-V_1 \frac{dp_1}{dt} - S_1(P_1)P_1 + q_1(t_1)F_1 + Q_1 = 0. \quad (2.1)$$

The end result of modelling the pumping is graphically presented in a logarithmic scale. The obtained graphic was divided in two parts to show pressure changes depending on pumping time in greater detail. The first part is more likely to characterize the first 60 seconds of pumping process, where pressure change curve and pump transition stage can be clearly seen in Fig. 2.2.

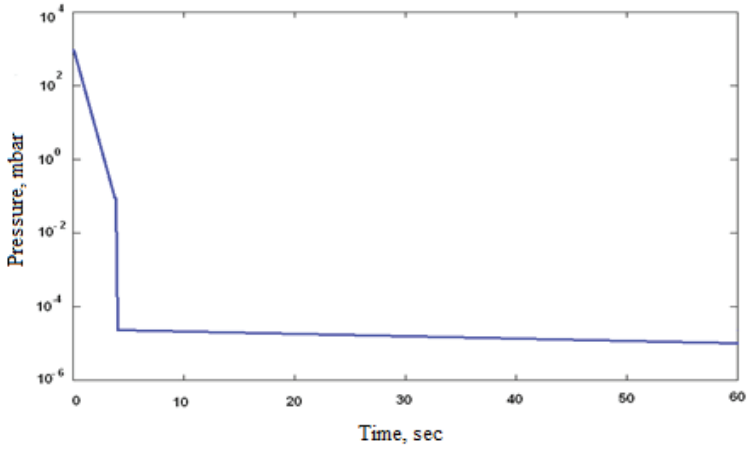

Fig. 2.2. Pressure changes in the first 60 seconds from start of pumping.

The simulation shows how long it takes to reach the base pressure; the operational auxiliary time of the pump is neglected in this example. This mathematical modelling helped to choose a proper pump and allowed to achieve the desired operational parameters of vacuum testing device.

2.4. Analysis of the main criterion of technological nanolayer process of vacuum device

Before the beginning of a technological nanolayer fetch-up process in vacuum chamber, one must check the pressure readings. Before I describe the experimental process and gained results, I would like to present an example that reviews the problems that I face in practice very often when performing nanolayer deposition. For nanolayer deposition UV 80 laboratory vacuum device was used, which was connected with three vacuum gauges, two of which were important: INFICON HPG 400 ionization vacuum gauge that can be seen as device 2, and CDG 025D diaphragm vacuum gauge that can be seen as device 3 in Fig. 2.3. (Figs. 2.3 and 2.4). In most cases it is sufficient to use CDG measurements, because these results are not dependent on gas, they are precise and the results are replicable [7].

Fig. 2.3. Ionization vacuum gauge HPG 400 pressure measurements with argon correction.

Fig. 2.4. Ionization vacuum gauge HPG 400 pressure measurement without argon correction.

In both cases argon is delivered into chamber, and the only thing that is changed is setting argon correction for vacuum gauge. Argon flow that is delivered to vacuum chamber is 14.4 % or 100 sccm [26]. Device HPG 400 without adjusted correction is showing the results that are closer to those of CDG measurement, though it should be the other way round. In this case, if we want to compare measurement without correction 8.58×10^{-4} Torr to 6.88×10^{-4} Torr, it is necessary to lower the argon flow to 11.2 % or 78 sccm [24], [26]. With the given data we conclude that argon difference is 22 sccm if we equate pressure measurements. Because of pressure measurement mutual error, it is harder to choose a more precise device for nanolayer deposition technological process. This example shows that regardless of comparing the measurements of both devices in order to increase or decrease the level of argon, the end result is not satisfactory because much more argon is used in the beginning and end of technological process than it is necessary.

3. TESTING OF VACUUM GAUGES USING MULTIFUNCTIONAL METHODS

3.1. Testing of ionization vacuum gauge using experimental vacuum device

First experiments aim to test three different ionization vacuum gauges and to gain a measurement precision overview, as well as to analyze error values.

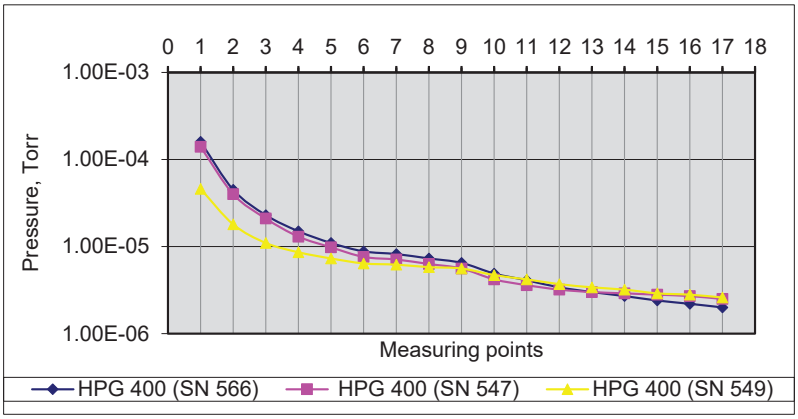

Fig. 3.1. Comparison of HPG 400 ionization vacuum gauge precision.

Experimental data that are presented in Fig. 3.1. show that vacuum gauge measurements are dissipated. Ionization vacuum gauge HPG 400 (SN 549) that had been used in a laboratory device showed greater error than other vacuum gauges.

According to vacuum gauge HPG 400 technical passport, the device should be able to measure pressure correctly within 2×10^{-6} mbar, which in turn indicates that error will grow when coming closer to measurement range limits.

The performed experiment showed that HPG 400 (SN 549) vacuum gauge measurements most significantly differed from the other measurement devices at points 1 to 9 and later evened out. Mean pressure measurement range that could show most precise values is located between 2×10^{-3} Torr and 2×10^{-4} Torr.

Measurement error for ionization vacuum gauge HPG 400 (SN 547) in both measurement points is in the range of 10 %–15 %. In case of HPG 400 (SN 549) measurement error in the same points is 71 % at the first, and 34 % at the second point. Thus, one can conclude that ionization vacuum gauge HPG 400 (SN 549) pressure measurements are far too imprecise and are far out of the allowed error range of ±15 %. The error can be related to many factors, e.g. total operation time, working environment, technological process, materials used in smearing process, pollution in sensing element area, and other factors.

After comparing the three vacuum gauges, it was concluded that valid measurement devices are SN566 and SN 547 vacuum gauges when comparing three vacuum gauges. On the other hand, the device with SN 549 is not correct and does not satisfy quality demands.

3.2. Testing of HPG 400 and BPG 402 ionization vacuum gauge using a new experimental vacuum device

Next step in overall process was to test a HPG vacuum gauge with BPG ionization vacuum gauge that has a wider measurement range. During experiments, it was assumed that the BPG device is more precise. After ten identical experiments, average pressure values were acquired. The results of experiment can be seen in Fig. 3.2.

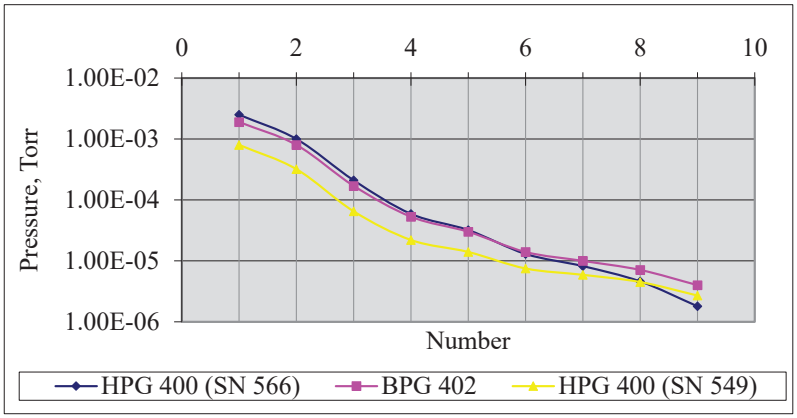

Fig. 3.2. Ionization vacuum gauge pressure curves.

Based on the obtained results, one can conclude that BPG and HPG (SN 566) vacuum gauges at low pressure value show similar results, whereas SN 549 is significantly different. As the measurement threshold approaches, in high vacuum, measurements between SN 566 and SN 549 begin to gradually equalize, but this is of little importance because the error of ±15 % is granted only until 10^{-5} mbar.

BPG vacuum gauge measurement range is from 10^{-2} mbar $- 10^{-8}$ mbar. HPG vacuum gauge reading range differs minimally but it was not found when measuring all three HPG devices. Based on result analysis, one can conclude that pressure measurement error of ionization vacuum gauge BPG 402 and BPG 400 (SN 566) does not exceed 15 % limit. It can be assumed that a correct pressure value is not related to a more accurate device, but based on ionization vacuum gauge experimental research, can be located in the trust interval of vacuum gauge pressure readings.

Testing of HPG 400 and BPG 402 ionization vacuum gauge with argon gas flow

During this experiment, argon is delivered into vacuum tank in different portions and the only thing that is manipulated is ionization vacuum gauge correction measurement against argon.

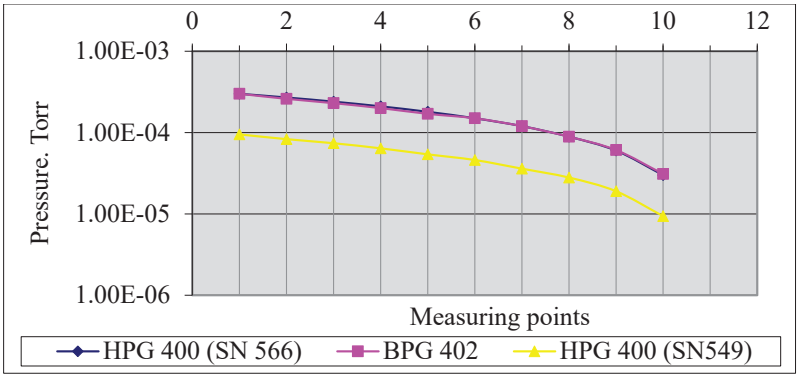

Fig. 3.3. Pressure curves of ionization vacuum meter experimental testing.

It is possible to compare the readings of HPG and BPG 402 device because the correction is turned off and normal device operation is not disturbed. The range that was chosen in the experiment was suited for BGP 402, so its results would be most precise amongst all other devices, thus ensuring excellent results and measurement differences. From these results one can conclude that device HPG 400 (SN 566) that was most precise of all HPG 400 group is showing readings that are very close to BPG 402 and the error is within 3.8 % tolerance, and in some points, is exactly the same at certain dosage of argon gas. On the other hand, HPG 400 (SN 549) is showing significantly different readings from BPG 402 and HPG 400 (SN 566), which was expected. SN 549 results against BGA 402 are presented in Fig. 3.3.

3.3. Using diaphragm type vacuum gauge for HPG 400 ionization vacuum gauge testing

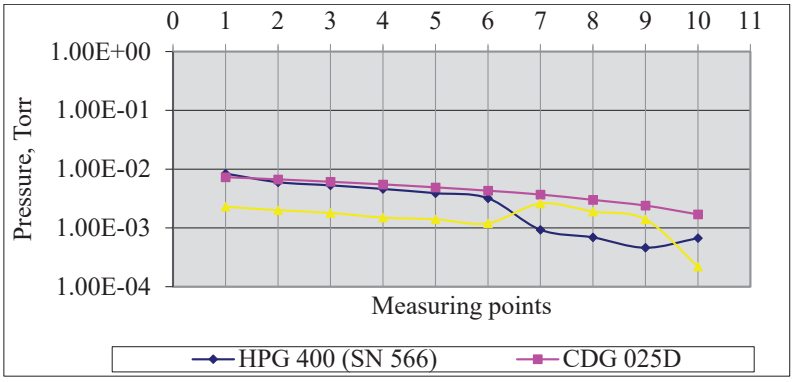

Fig. 3.4. Vacuum gauge pressure experimental curves with argon correction.

Diaphragm type device is considered to be the most precise of available batch of measurement devices used in experiments because of its operation and the fact that the gas flow is not affecting readings, precision is tolerated between 0.2−0.5 % from measurement value [33], [22], [15], [37]. It is adapted for usage in technological process of SiO_2 nanolayer

deposition. Ionization vacuum gauges are tested in relation to CDG 025D in order to test pressure ranges at low and medium vacuum.

The comparison of results for HPG 400 (SN 566) and CDG 025D with 10 sccm argon in chamber are presented in Fig. 3.4. First six readings are pretty close, and the tolerance for HPG device is within 15.5 %. Further readings considerably exceed 15 % error tolerance. In Fig. 3.4., we can see that that there is a considerable drop that appears at 4–1 sccm. There is no clear answer why HPG 400 (SN 566) curve abruptly drops from 4 sccm to 1 sccm, thus showing better vacuum than there actually exists, but at 1 sccm rises again showing a worse degree of vacuum. One of the reasons could be that the hot cathode ionization of vacuum gauge turns on at a certain pressure value; according to the technical data of the device, this turn on point can be varied as desired. In addition, ionization switchover is possible from 1 mbar to 5×10^{-2} mbar that does not correspond to a particular vacuum gauge bump and vacuum changes in a particular pressure range. HPG 400 SB 566 and SN 547 vacuum gauges are set to switch to a hot cathode from 1 mbar. Graphically all SN 547 readings differ at all points and show a better degree of vacuum than other vacuum gauges. While CDG device readings are as expected, there are abrupt pressure changes for the gas flow of 4–1 sccm argon on ionization device readings.

3.4. Gas correction effect on vacuum gauge readings

The equation of ionization vacuum gauge gas correction is the following [27], [44]:

$$P_{eff} = K \times P_{diff}, \tag{3.1}$$

where K = 0,8 (for argon).

Table 3.1.

Comparison of Measured and Calculated Pressure of Ionization Vacuum Gauge

No.	Argon flow, sccm	With argon in chamber, without correction (SN547), Torr	Calculated pressure value (SN547), Torr	With argon in chamber and correction (SN547), Torr	Error, %
1	10 sccm	3.00E-03	2.40E-03	2.30E-03	4.20 %
2	9 sccm	2.60E-03	2.08E-03	2.00E-03	3.80 %
3	8 sccm	2.30E-03	1.84E-03	1.80E-03	2.20 %
4	7 sccm	2.10E-03	1.68E-03	1.50E-03	1.70 %
5	6 sccm	1.80E-03	1.44E-03	1.40E-03	2.80 %
6	5 sccm	1.50E-03	1.20E-03	1.20E-03	0 %
7	4 sccm	1.20E-03	9.60E-04	2.60E-03	171 %
8	3 sccm	2.50E-03	2.00E-03	1.90E-03	5 %
9	2 sccm	1.70E-03	1.36E-03	1.40E-03	2.90 %
10	1 sccm	2.70E-04	2.16E-04	2.20E-04	1.90 %

The results obtained from ionization vacuum gauge with correction differed from the results that were calculated based on pressure without correction. The results were compared, and relative error was calculated. Percentage error can be seen in Table 3.1. The experiments led to the conclusion that there are abrupt pressure reading changes when the gas flow is 4 sccm. If these readings are not taken into consideration, the shown quality and error tolerance is 4.2 %.

While testing ionization vacuum gauge HPG 400 correction after argon flow delivered to the chamber, it was concluded that the calculated pressure value and correction differ. The accuracy error calculated between the calculated and the displayed value was calculated as a percentage. Ionization vacuum gauges have documented error tolerance, besides that ionization vacuum gauges have correction depending on gas and this correction is delivered with an additional error. By summing up both factors, we can assume that the error in particular ranges is considerably affecting vacuum gauge precision.

3.5. Testing of BPG 402 ionization and high precision diaphragm vacuum gauge

During HPG 400 tests, two more precise vacuum gauges were used that operated in different pressure ranges. HPG 400 ionization vacuum gauges were tested in different pressure ranges and at different gas flow volumes. CDG vacuum gauge was chosen as the most precise device for pressure readings from 1×10^{-4} Torr to 0.1 Torr. On the other hand, BPG 402 ionization vacuum gauge was chosen as the most precise device for high vacuum range until 2×10^{-6} mbar.

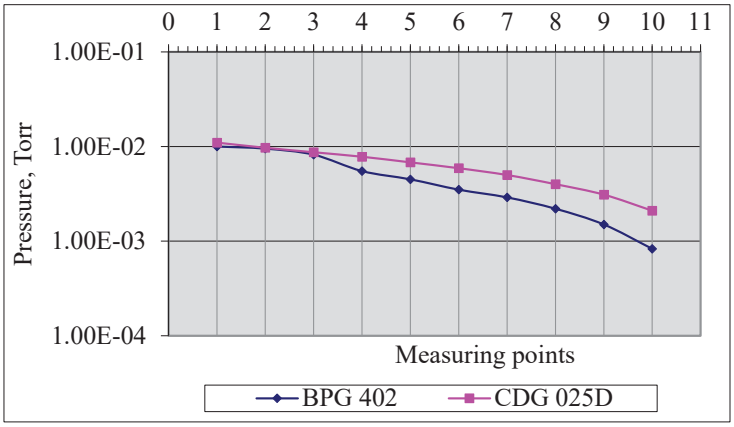

Fig. 3.5. Vacuum gauge experimental pressure curves.

From gained experimental results presented in Fig. 3.5. it can be concluded that pressure readings CDG and BPG vacuum gauge differ. The highest difference was observed when argon gas of 1 sccm was delivered to chamber and the error reached 60.5 %. During all readings, CDG device showed worse degree of vacuum than the BPG type device. Thus, we conclude that gas correction can affect measurement precision.

3.6. Experimental research on diaphragm vacuum gauge and gas impact

During the experiment, the vacuum chamber was pumped and then argon gas was delivered in maximum allowable amount, in our case it was 150 sccm. After this volume of gas had been delivered into the chamber, pressure was set closer to the value of 9×10^{-3} Torr, so the

vacuum gauge was tested at a range where it is most often used in technological process and experiments. During experiments both argon and oxygen was delivered to chamber in different volume as mixture and separately, too. The goal of this experiment was to test vacuum gauge precision and effect of gas on the vacuum gauge precision.

Table 3.2.

Measured Diaphragm Vacuum Pressure Error Depending on Gas Volume

No.	With, sccm	O_2, sccm	CDG 025D, Torr	Error, %
1	50	50	6.22E-03	Output data
2	75	25	6.44E-03	3.54 %
3	25	75	6.02E-03	3.22 %
4	0	100	6.02E-03	3.20 %
5	100	0	6.65E-03	6.90 %
6	75	75	9.15E-03	Output data
7	50	100	8.94E-03	2.30 %
8	100	50	9.30E-03	1.64 %
9	150	0	9.73E-03	6.30 %
10	0	150	8.76E-03	4.30 %

The obtained data shows that when keeping the total gas amount of 100 sccm in the chamber while at the same time changing argon and oxygen proportions, CDG device pressure readings are changing (Table 3.2.). Data shows that diaphragm gauge measuring speed changes with the gas volume. The experimental data show that the measurement error reached 6.90 %.

Pumping speed is a variable value, but it can stay constant when it reaches certain values. For example, see typical pumping velocity curves of turbomolecular pump TURBO–V3K–T in Fig. 3.6. [41].

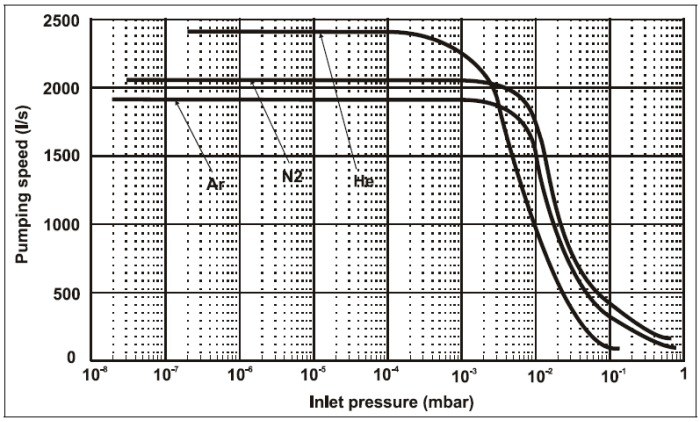

Fig. 3.6. Pumping velocity curves of turbomolecular pump.

Looking at argon curve it can be defined that in the range of 0.1–0.01 mbar pressure, pumping speed is leveling out to a flat constant and remains unchanged until 5×10^{-7} mbar [27].

The pressure can be calculated as follows:

$$P = \frac{Q}{S}, \tag{3.2}$$

where Q is gas flow (sccm), $\text{sccm} = 0{,}0127\frac{\text{Torr}\cdot\text{l}}{\text{s}}$ (Appendix 2); S is pumping velocity (l/s); and P is pressure (Torr).

Table 3.3.

Numerical Values of Diaphragm Vacuum Gauge Pressure Measurement Error

No.	With, sccm	O2, sccm	Measured pressure CDG 025D, Torr	Calculated pressure, Torr	Error, %
1	50	0	2.86E-03	Output data	0 %
2	0	50	2.64E-03	2.86E-03	7.70 %
3	0	100	5.15E-03	5.72E-03	9.97 %
4	100	0	5.75E-03	5.72E-03	0.52 %
5	75	0	4.33E-03	4.29E-03	0.93 %
6	0	75	3.94E-03	4.29E-03	8.16 %
7	150	0	8.52E-03	8.58E-03	0.70 %

Experimental results are shown in Table 3.3. If vacuum chamber is receiving only argon gas, then 50 sccm is considered to exit reference point. Then based on the obtained calculations, one can compare different measurement points. Thus, increasing argon gas flow by 25 % and by 100 % we gain pressure values that differ by 0.93 % and 0.52 %. This kind of device operation is considered normal and is within measurement error tolerance of 1 %. Keeping in mind that there may be situations when the measured pressure values are far outside of the expected value range, e. g. when vacuum chamber is filled with 100 sccm oxygen, measurement error against the calculated value is 9.97 %.

3.7. Experimental research on diaphragm vacuum gauge before and after zero adjustment

Using a new experimental vacuum device, zero point adjustment was accomplished to a diaphragm vacuum gauge. This zero point can drift in case of pollution or long workload; then zero point needs to be adjusted to ensure the quality demands.

Table 3.4.

Measured and Calculated Pressure of Diaphragm Vacuum Gauge Before Zero Adjustment Operation

Argon flow, sccm	Measured pressure CDG 025D, Torr	Calculated pressure, Torr	Error, %
10 sccm	7.30E-03	1.7E-02	132.88 %
8 sccm	6.10E-03	1.36E-02	122.95 %
6 sccm	4.90E-03	1.02E-02	108.16 %
4 sccm	3.70E-03	6.8E-03	83.78 %
2 sccm	2.40E-03	3.4E-03	29.41 %
1 sccm	1.70E-03	Output data	0 %

By reviewing Table 3.4., we can conclude that at a higher argon gas flow the pressure difference between experimental and calculated values is below 1%, whereas, when replacing argon with oxygen, the pressure error between the calculated and measured result reaches 9.97 %. Thus, we can conclude that the adjustment of zero point for diaphragm vacuum gauge is partly successful, because when working with argon gas and changing gas volume, pressure reading is changing accordingly within the allowed tolerance; whereas in case of substituting argon with oxygen or mixture of both, this error is far higher than expected and exceeds the allowed 1% of tolerance.

3.8. Gass flow controller precision experiments

Vacuum system consists not only from a pressure measurement device but also contains mass flow controller (MFC) that is responsible for controlling how much gas is delivered in chamber, which is a common practice during magnetronic smearing. During the experiment, a certain amount of gas was delivered to the chamber.

Table 3.5.

Diaphragm Vacuum Gauge Pressure Error Using Oxygen MFC

No.	With (sccm)	CDG 025D (Torr)	CDG 025D (Torr) through oxygen MFC	Error
1	50	3.40E-03	3.58E-03	5.00 %
2	75	5.00E-03	5.26E-03	4.94 %
3	100	6.68E-03	6.92E-03	3.47 %
4	150	9.83E-03	1.00E-02	1.70 %

Delivery of argon gas was done with particular argon MFC, whereas oxygen delivery to vacuum chamber was done through oxygen chamber. When both argon and oxygen gas MFCs were working together, the maximum value of calculated and experimentally obtained reached the error of 5%. As seen in Table 3.5., we can conclude that argon gas flow separately and through oxygen MFC is being delivered in proper amount, because when comparing both results, we can see that mutual pressure difference is not greater than 5 %, and with an increasing argon gas proportion this error has a tendency to drop. MFC works well but with slight offsets, not exceeding 5%. Pressure measurement error is related to the diaphragm vacuum gauge itself and possibly to other conditions.

3.9. Vacuum gauge testing using Student's distribution

By Student's distribution, it is possible to check the vacuum gauge reading dispersion, calculate mean square error as well as mean reliability interval (Table 3.6.) [27].

Table 3.6.

Diaphragm Vacuum Gauge Pressure Units Using Oxygen MFC

n	HPG 400 Measured pressure x_i, Torr	$\Delta x = \bar{x} - x_i$, Torr	Δx^2, Torr
1	3.99E-04	+ 0.11E-04	0.0121E-04
2	4.11E-04	+ 0.001E-04	0.0001E-04
3	4.25E-04	+ 0.15E-04	0.0225E-04
4	3.80E-04	– 0.3E-04	0.09E-04
5	4.15E-04	+ 0.05E-04	0.0025E-04
6	4.22E-04	+ 0.12E-04	0.0144E-04
7	4.51E-04	+ 0.41E-04	0.1681E-04
8	4.35E-04	+ 0.25E-04	0.0625E-04
9	3.91E-04	– 0.19E-04	0.036E-04
10	3.86E-04	– 0.24E-04	0.0576E-04

Calculation of root mean square error (RMS) [27]:

$$S = \sqrt{\frac{\sum_i^n (x_i - \bar{x})^2}{n-1}} = 0{,}227\text{E} - 04 \text{ Torr}. \quad (3.3)$$

Using the Table given in Appendix 1, we defined Student's coefficient $f = n - 1 = 9$; (P = 0.95) t = 2.26, and calculated reliability interval of mean value [27]:

$$\Delta\bar{x} = \sqrt{\frac{S^2}{n}} = \frac{S}{\sqrt{n}} = \frac{2{,}26 \times 0{,}227}{\sqrt{10}} = 0{,}16223\text{E} - 04 \text{ Torr}. \quad (3.4)$$

Then mean value interval of pressure is $4{,}1 \pm 0{,}16\text{E} - 04$ Torr [27].

Experimental values obtained in the experiment do not cross the allowed interval border from 4.05E–04 Torr ±15 %; vacuum gauge precision while manipulating with oxygen flow and holding starting pressure is acceptable. Measured pressure values are both negative and positive, and calculated mean value is close to the starting pressure.

4. IMPACT OF PRESSURE ON VACUUM NANOLAYER PROPERTIES AND VISUAL PROPERTIES

4.1. SiO2 vacuum device for nanolayer deposition and its construction

Many experiments were conducted using device UV80 at "Sidrabe", Inc., which concentrated on SiO_2 nanolayer fetching onto film at different pressure levels with the aim to obtain data showing general quality and overall properties of nanolayer (Fig. 4.1.). The laboratory device is suitable for metal and oxide magnetronic smearing on sheet and roll type materials such as film, fabric and metal foil.

Applicable roll type films have the following properties:

1) maximum possible width of film is 600 mm, but fetch on nanolayer width is changeable with protective screens within limits of 200 to 550 mm [13];
2) allowed film thickness is 50 to 200 μm;
3) maximum possible length of film is 500 m, depending on its thickness.

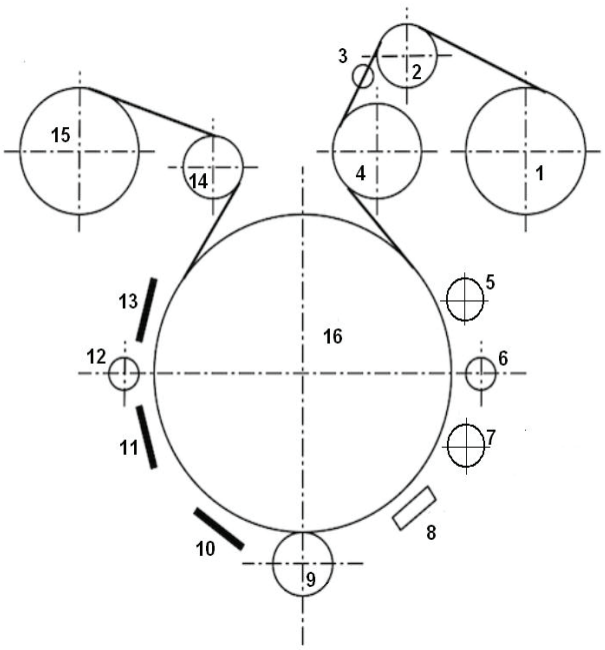

Fig. 4.1. Principal diagram of vacuum device UV80 rewinding mechanism:
1, 2, 4, 14, 15 – rolls; 16 – main barrel; 3 – light transparency measurement device; 5, 7 – planar magnetrons; 6, 12 – gas inputs; 8 – ion cannon; 9 – press-roll; 10 – glow discharge device; 11, 13 – magnetrons.

Vacuum device UV80 is equipped with both ion cannon and glow discharge device, thus supporting foundation preprocessing before nanolayer deposition. The main barrel is used for the drying and degassing process of this foundation where it is heated to 90 °C temperature.

4.2. SIO2 nanolayer deposition experiments

Experiments were conducted using laboratory device UV80. PET film was used as a foundation with a fetch-on zone width of 500 mm and length of 2 m of each sample. Impulse DC power supply Advanced Energy Pinnacle Plus, 10 kW Pulsed DC, 0–350 kHz was used in this experiment with one magnetron where silicon was used as target material. SiO_2 nanolayer was chosen for the experiment because of its main property – increasing light transparency.

The aim of these experiments was to evaluate the effect of different pressure changes on nanolayer properties such as light transparency and thickness of nanolayer, as well as its visual status.

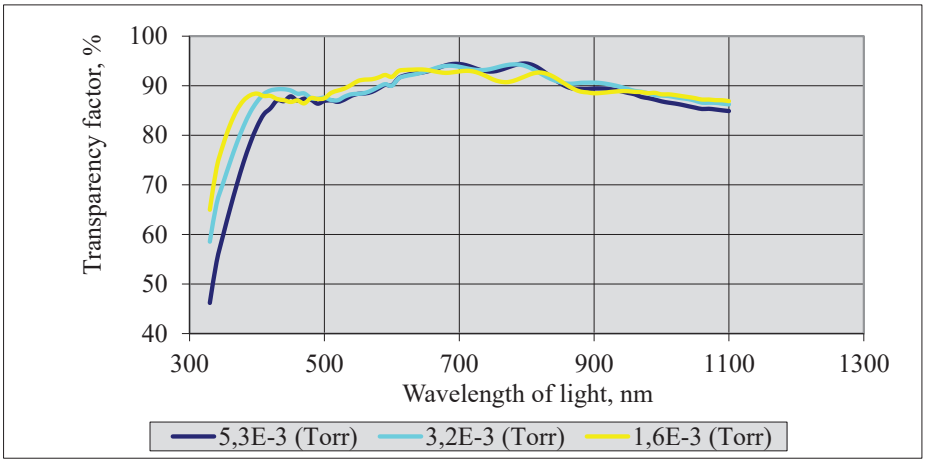

Fig. 4.2. Light transparency curves of three SiO_2 nanolayers.

Light transparency of all three nanolayer samples exceeds 88 %, which had been set as a limit based on PET film transparency properties (Fig. 4.2.)

Table 4.1.

Numerical Values of SiO_2 Nanolayer Thickness and Transparency Factor

Pressure, Torr	Mid of foundation		Side of foundation	
	Thickness, nm	Transparency factor, %	Thickness, nm	Transparency factor, %
5.3E-03Torr	348.3	88.37	359.8	87.42
3.2E-03 Torr	362.5	88.37	349.4	88.28
1.6E-03 Torr	334.4	90.98	327.4	90.87

Experimental results are presented in Table 4.1. The samples have visual difference at different wavelengths at 3.2×10^{-3} Torr and 5.3×10^{-3} Torr, although their transparency factors are the same. The nanolayer that was obtained at 5.3×10^{-3} Torr pressure was darker at ultraviolet zone and had lower transparency factor than the sample taken at 3.2×10^{-3} Torr. It means that the pressure that was achieved in the chamber is related to nanolayer quality and

properties; in the given example it is light transparency factor. It is important to pay attention to the thickness of nanolayer as well.

Nanolayer transparency at different pressures of 5.3×10^{-3} Torr and 3.2×10^{-3} Torr is the same, but their thickness differs by 13.9 nm. The nanolayer with highest thickness is only 334.3 nm thick. By using the software provided by company FILMETRICS it was possible to check the dependence of nanolayer reflection factor on thickness material (Fig. 4.3.) [43].

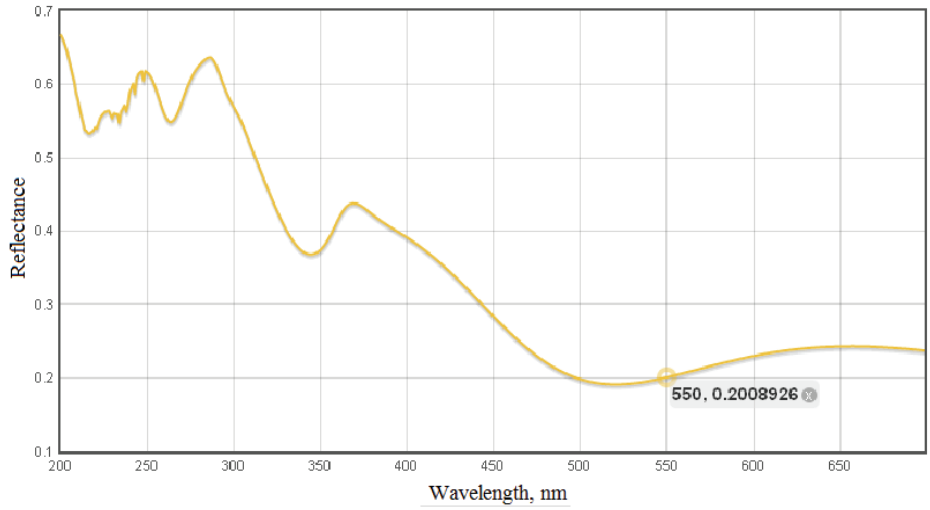

Fig. 4.3. Reflection factor at different wavelengths of SiO_2 nanolayer with thickness of 348.3 nm (taken at 5.3×10^{-3} Torr).

Light reflection factor is dependent on thickness of the material. Thicker materials have lower reflection values. The obtained nanolayer samples were tested, analyzed and described, a simulation was done using the provided online software. From research results, one can conclude that process management and nanolayer deposition at different pressures affect the sample properties and visual status. It is possible to obtain feasible SiO_2 nanolayer properties, thickness and visual condition at the pressure of 1.6×10^{-3} Torr if a process control is maintained in transition zone.

If the pressure limits are changed, nanolayer properties are changing, therefore the process needs a precise and reliable pressure measurement device. Pressure changes can oscillate in different ranges depending on situation as well as on erroneous behaviour of the measurement device. Not only the visual state of the nanocoating can change; depending on the operation of the elements of the device and other process conditions, the homogeneity of the nanolayer can change along the entire length of the base.

5. PREDICTION OF SiO2 NANOLAYER TRANSPARENCY AND THICKNESS USING FUZZY LOGIC

5.1. Basics of fuzzy logic and its experimental application

In order to simulate systems more precisely and more comprehensively it is suggested to change the approach from using numerical and binary methods to linguistic methods, which gives the possibility to use not only numerical values but also words and whole sentences as well [2], [38]. Those are elements of fuzzy logic. Latvian Academy of Sciences is defining fuzzy logic as logic that has been developed to better present knowledge and human thinking. Fuzzy logic is widely used in such fields as artificial intelligence (AI) robotics, and information technologies. The difference from binary logic is that a defined range of values is not limited to 0 or 1 (true, false), but reaches out further defining "true", "false", "more or less true", "almost true", "totally false", "almost false", "very false", which makes it closer to human thinking [48].

In other words, fuzzy logic has been developed to approximate human thinking and analysis process [15]. Fuzzy logic gives a chance to predict the main result and develop prediction model based on input data [22], [37]. Fuzzy logic allows to present human decision and situation analysis process in algorithmic form [39]. If traditional binary logic is operating with two values (true or false) then fuzzy logic has far more options, for example: "true", "false", "not true", "more or less true", "false", "very true" that makes it closer to human thinking.

Two main process parameters are described with fuzzy logic and linguistic formulation: gas flow volume (changing input values) and transparency factor (changing output value). Graphically linguistic variables are presented as surfaces with modest borders, whereas numerical variables are presented as dots in surface. Fuzzy logic model is based on basic principle "if – then" that describes mutual relation of variables. The obtained result is presented as 2D or 3D visualization graphic that describes changes of parameter mutual effect as well as gives an opportunity to analyze particular zones where it is feasible or not feasible to perform the technological process to obtain the related parameters [16].

5.2. Development of SiO2 nanolayer transparency and thickness fuzzy logic models

To obtain data, experiments with SiO_2 nanolayer deposition were conducted using laboratory device UV80; SPEKTROMETRS MC 122 ("Sidrabe", Inc.) was used to measure transparency coefficient, whereas nanolayer thickness was measured with FILMETRICS F20-UV ("Sidrabe", Inc.) [25]. The fuzzy logic model was developed with a special software programme fuzzyTECH 8.30.b Professional Demo.

Two input and output parameters were used in the development of fuzzy logic model, for input – volume of oxygen flow and volume of air flow, for output – transparency factor and thickness of nanolayer (Fig. 5.1.) [25].

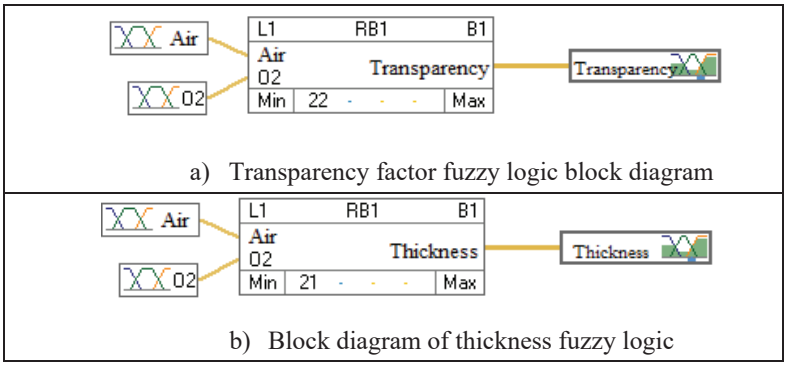

Fig. 5.1. Fuzzy logic block diagrams.

Each parameter was given a fuzzy logic group with belonging functions with values within the range from 0 to 1. Belonging functions were the same for transparency and thickness fuzzy logic model. Air, oxygen, transparency and thickness values were grouped under five belonging functions. Conditions were set for nanolayer thickness and transparency blocks.

5.3. Data de-fuzzyfication and prediction models

Data de-fuzzyfication was done and prediction models were obtained that are presented as 3D graphics in Figs. 5.2. and 5.3 [25]. The main aim of SiO_2 experiments was to obtain a fuzzy logic prediction model for nanolayer transparency factor and thickness simulating drain during the technological process.

These models allow us to predict possible light transparency factor and material thickness depending on drain volume and make a decision to continue or to stop the technological process for the nanolayer properties to be compliant to quality demands [25]. In case of drain, prediction models allow to predict particular transparency factor and related thickness area and to achieve gas correction in the desired direction.

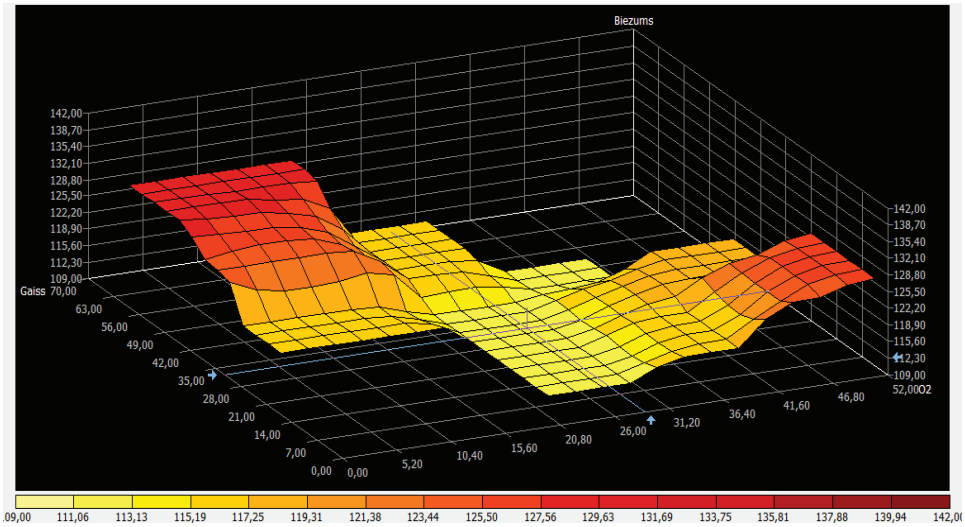

Fig.5.2. 3D fuzzy logic program model of thickness.

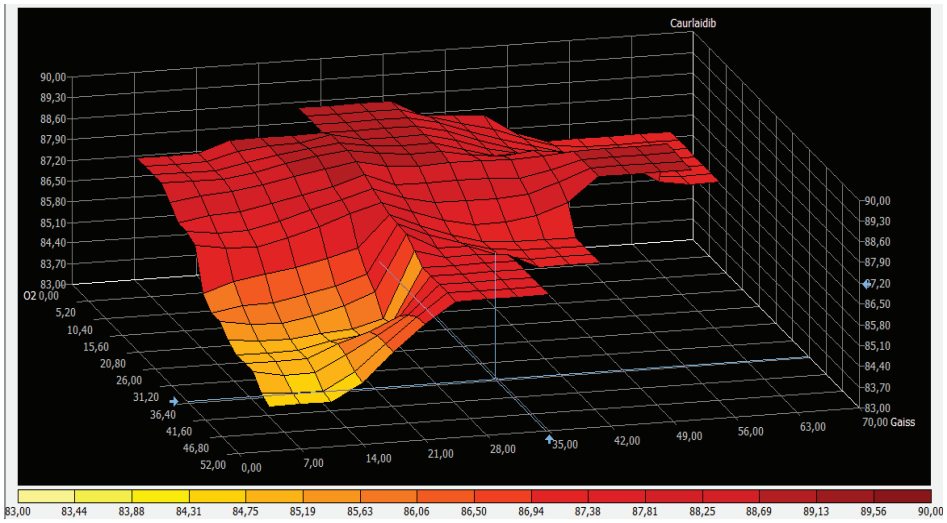

Fig. 5.3. 3D fuzzy logic program model of transparency factor.

By changing input parameter values, software and fuzzy logic is allowing to determine and predict nanolayer transparency factor and thickness. By using fuzzy logic and program models it is possible to decrease the number of nanolayer deposition experiments, take the decision to stop the technological process or to make some parameter adjustment with the aim to obtain satisfying nanolayer properties [3].

6. DEVELOPMENT OF METHODOLOGY FOR VACUUM GAUGE TESTING

Based on vacuum techniques, new vacuum equipment, vacuum gauge operating principle and behavioural analysis, as well as on all the performed and described experiments, a vacuum gauge testing methodology was developed (Fig. 6.1.). The diagram of the vacuum gauge testing block depicts the most important stages of technological process, by following which it is possible to switch off the device and to adjust it, as well as to ensure, to control and to set the nanolayer deposition. The developed vacuum gauge testing methodology allows to investigate the performance nuances, accuracy, behaviour at various changing conditions, and to find the most appropriate vacuum gauge application based on the pressure range, environment and other factors that influence the measurements. The obtained experimental results can be collected and used as a database.

Precision and result replicability of the tested vacuum gauge may stay the same as before experimental tests using the developed testing methodology, but the obtained data allows us to analyze the vacuum gauge precision in different pressure ranges. This is the reason why during nanolayer vacuum deposition technological process with imprecise measurement device we can include a correction factor based on experimental test data, as well as include the correction factor for the parameters of nanolayer deposition process.

During the doctoral research, a testing of diaphragm type vacuum gauge was conducted as well as zero adjustment and data collection. Based on the data presented in Table 3.3., it is possible to approximately calculate a diaphragm vacuum gauge error during SiO_2 nanolayer deposition process. The predicted error will be in the range from 7.70 % to 9.19 %. For SiO_2 technological process, this error is in an acceptable range, which is not affecting nanolayer transparency, thickness or visual status.

Vacuum gauge test can be done periodically, thus gaining new data and analyzing them, developing a behavioural model of vacuum gauge pressure change and thus adjusting the device for the nanolayer deposition process. This test is also needed to avoid the decision to send the device for recalibration in a specific laboratory. Vacuum gauge test does not exclude an option of instrument calibration but allows to analyze the need for such operation. Vacuum gauge testing methodology is unique and contains multiple test methods, gives chance to research vacuum gauge operation and collect results, thus allowing to develop a correct model.

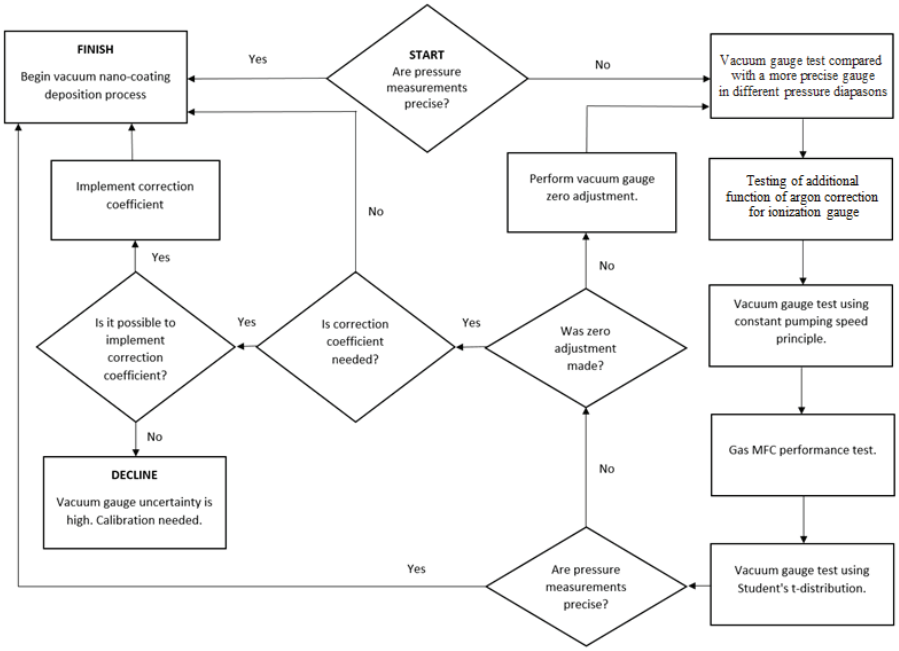

Fig. 6.1. Vacuum gauge testing methodology.

CONCLUSIONS

1) After advantage and disadvantage analysis, a conclusion has been drawn that for low vacuum most precise device would be a diaphragm type vacuum gauge, due to its simple construction, result replicability, and resistance against different gas environments.
2) A special experimental vacuum test device has been engineered and produced that allows to achieve 2×10^{-6} Torr vacuum in a very short time period (approximately 20 min).
3) A series of multifunctional experimental research has been conducted on vacuum devices HPG 400, BPG 402, and CDG 025D using laboratory equipment UV80 and a newly produced experimental test device. During research ionization, vacuum gauge gas correction functions as well as the condition of gas flow measurement device were tested. Before the experimental test, the diaphragm vacuum gauge error exceeded the allowed relative error value of 0.2 % and in few particular cases reached an error level of 132.88 %. After zero adjustment and repeated experimental test, maximal relative error decreased to 9.97 %. Based on vacuum gauge experimental results and fetch-up experimental results, it was concluded that the predicted error of diaphragm vacuum gauge after test manipulations can be in the range from 7.7 % to 9.19 %. This error level does not considerably affect the visual condition and properties of nanolayer.
4) Pressure oscillation affect on nanolayer properties and visual condition were researched. For these experiments, SiO_2 nanolayer was chosen as well as laboratory device UV80. The obtained results showed that small pressure oscillations may affect nanolayer properties and visual condition, thus a nanolayer with best transparency factor of 90.98 %, reflection factor 0.2433, and visual condition was fetched up at $1.6 \cdot 10^{-3}$ Torr. Whereas the nanolayer sample fetched up at $5.3 \cdot 10^{-3}$ Torr, had more metal phase signings (dark brown color) and a light transparency of 87.42 %.
5) A fuzzy logic model was developed for SiO_2 nanolayer transparency and thickness prediction in case of drain that allows predicting of the nanolayer transparency factor and thickness. By using fuzzy logic and prediction models it is possible to decrease the needed nanolayer fetch-up experiment count, make a decision to stop the technological process or to adjust some parameters in order to achieve satisfying nanolayer properties and continue the technological process.
6) Based on vacuum test and nanolayer fetch-up experiments conducted during the doctoral research, as well as on other specifics of nanolayer fetch-up process in company “Sidrabe” Inc., a new vacuum device testing methodology was developed for vacuum nanolayer fetch-up process with the aim to ensure the possibility to research vacuum gauge operation, precision, result replicability, and behaviour in changing conditions, as well as to perform zero point adjustment, implement and support data base, implement correction factor based on experimentally obtained data, and to support fast and handy vacuum gauge testing method.

REFERENCES

1. Akram, H. M., Fasih, A. Selection Criterion of Gauges for Vacuum Measurements of Systems with Diverse Ranges. *Physics Procedia*. 2012, Vol. 32, pp. 503–512. Available from: doi: 10.1016/j.phpro.2012.03.594.
2. Athanasopoulos, G., Riba C. R., Athanasopoulou, C. A decision support system for coating selection based on fuzzy logic and multi-criteria decision making. *Expert Systems with Applications*. 2009, Vol. 36, No. 8, pp. 10848–10853. Available from: doi: 10.1016/j.eswa.2009.01.016.
3. Barzani, M. M., Zalnezhad, E., Sarhan, Ahmed A. D., Farahany, S., Ramesh, S. Fuzzy logic based model for predicting surface roughness of machined Al–Si–Cu–Fe die casting alloy using different additives-turning. *Measurement*. 2015, Vol. 61, pp. 150–161. Available from: doi: 10.1016/j.measurement.2014.10.003.
4. Bishop, C. A. *Vacuum deposition onto webs, films and foils*. Amsterdam: William Andrew Publishing, 2006, 497 p. ISBN: 978-0-8155-1535-7.
5. Daudé, B., Elandaloussi, H., Janssen, K. On the gas dependence of thermal transpiration and a critical appraisal of correction methods for capacitive diaphragm gauges. *Vacuum*. 2014, Vol. 104, pp. 77–87. Available from: doi: 10.1016/j.vacuum.2014.01.002.
6. Gavignet, E., Lanzetta, F. Dynamic operation of a micro-thermocouple sensor as a vacuum gauge. *Vacuum*. 2014, Vol. 100, pp. 18–21. Available from: doi: 10.1016/j.vacuum.2013.07.043.
7. Hidalgo, M. J., Segovia, J. L. De. Uncertainties in calibration using capacitance diaphragm gauges as reference standard. *Vacuum*. 2008, Vol. 82, No. 12, pp. 1503–1506. Available from: doi: 10.1016/j.vacuum.2008.03.092.
8. Hyland, R. W., Shaffer, R. L. Recommended practices for the calibration and use of capacitance diaphragm gages as transfer standards. *Journal of Vacuum Science & Technology A: Vacuum, Surfaces, and Films*. 1991, Vol. 9, No. 6, pp. 2843–2863. Available from: doi: 10.1116/1.577209.
9. Isogai, H. Analysis of thermal influence on the accuracy of a spinning rotor gauge. *Vacuum*. 1993, Vol. 44, No. 11–12, pp. 1181–1187. Available from: doi: 10.1016/0042-207x(93)90344-a.
10. Jitschin, W., Ludwig, S. Dynamical behaviour of the Pirani sensor. *Vacuum*. 2004, Vol. 75, No. 2, pp. 169–176. Available from: doi: 10.1016/j.vacuum.2004.02.002.
11. Jiang, F., Zhang, T. F., Wu, B. H., Yu, Y., Wu, Y. P., Zhu, S. F., Jing, F. J., Huang, N., Leng, Y. X. Structure, mechanical and corrosion properties of TiN films deposited on stainless steel substrates with different inclination angles by DCMS and HPPMS. *Surface and Coatings Technology*. 2016, Vol. 292, pp.54–62. Available from: doi: 10.1016/j.surfcoat.2016.03.007.
12. Jung, D. H., Moon, I. K., Yun, Y. J., Park, C. D., Chung, S. M., Jeong, Y. H. Measuring thermophysical properties of gases with a single thermocouple: Peltier vacuum gauge. *Thermochimica Acta*. 2007, Vol. 455, No. 1–2, pp. 40–45. Available from: doi: 10.1016/j.tca.2006.12.002.

13. Kazušs, J., Kozlovs, V., Mačevskis, E. *Processes Control for Oxide Layer Deposition in Roll-to-Roll Vacuum Machines* [online]. SVC, 2013 [Viewed 12 July 2017]. Available from: http://www.bing.com/cr?IG=20217DEB0D51462CB9E4FA180F609A98&CID=3C3E8112B9366CF129F78A5DB8306D68&rd=1&h=O5SmOFOwftu9ubSlCSmJ-gbOqOvJZ8Xqw-YK73yLBcQ&v=1&r=http%3a%2f%2fwww.sidrabe.com%2fassets%2ffiles%2fProcesses%2520Control%2520for%2520Oxide%2520Layer%2520Deposition%2520in%2520Roll-to-Roll%2520Vacuum%2520Machines_2013.pdf&p=DevEx,5067.1
14. Kocas, I., Sariyerli G. S. The characterization of new VGMS (vacuum gauge metrology system) by the traceability of multi stage static expansion system. *Measurement*. 2012, Vol. 45, No. 10, pp. 2430–2433. Available from: doi: 10.1016/j.measurement.2011.10.043.
15. Kromanis, A., Krizbergs, J. Prediction of 3D Surface Roughness Using Regression Analysis and Fuzzy Logic, and their Comparative Analysis. *Ražošanas tehnoloģija*. 2013, Vol. 35, pp. 130–137. ISSN 1407-8015. e-ISSN 2255-8721.
16. Kromanis, A., Krizbergs, J. Prediction of Surface Roughness in End-Milling Using Fuzzy Logic and Its Comparison to Regression Analysis. *Ražošanas tehnoloģija*. 2009, Vol. 31, pp. 75–78. ISSN 1407-8015.
17. Li, D., Jousten, K. Comparison of some metrological characteristics of hot and cold cathode ionisation gauges. *Vacuum*. 2003, Vol. 70, No. 4, pp. 531–541. Available from: doi: 10.1016/s0042-207x(02)00781-9.
18. Ma, G., Wang, L., Gao, H., Zhang, J., Reddyhoff, T. The friction coefficient evolution of a TiN coated contact during sliding wear. *Applied Surface Science*. 2015, Vol. 345, pp. 109–115. Available from: doi: 10.1016/j.apsusc.2015.03.156.
19. Murray, V.A.C. *VACUUM SCIENCE AND ENGINEERING*. New York: McGraw Hill, 1965. 239 p.
20. Odītis, I., Rudzītis, J. *Precizitāte un drošums 1.daļa*. Rīga: RTU izdevniecība, 2008. 115 lpp.
21. Pfeiffer Vacuum GmbH. *The Vacuum Technology Book Volume II Part 2 Know how book*. Asslar: Pfeiffer Vacuum GmbH, 2013. 140 p.
22. Sakthivel, G. Prediction of CI engine performance, emission and combustion characteristics using fish oil as a biodiesel at different injection timing using fuzzy logic. *Fuel*. 2016, Vol. 183, pp. 214–229. Available from: doi: 10.1016/j.fuel.2016.06.063.
23. Shao, A. L., Cheng, Y., Zhou, Y., Li, M., Xi, T. F., Zheng, Y. F., Wei, S. C., Zhang, D. Y. Electrochemistry properties of multilayer TiN/Ti coatings on NiTi alloy for cardiac occluder application. *Surface and Coatings Technology*. 2013, Vol. 228. pp. 257-261. Available from: doi: 10.1016/j.surfcoat.2012.05.129.
24. Stekleins, A., Gerins, E., Kromanis, A. *Analysis of selection criteria for vacuum gauges and its accuracy* [online]. Tallinn, 2016 [viewed 5 December 2017]. Available from: http://www.bing.com/cr?IG=B9514ADC68BC459AAC68CD00781DC610&CID=07B7D90498366CBB1607D24B99306D08&rd=1&h=bLtWL_qGHD0N9VfJxKMiaTSAZSVIzQdNasEn4BMCP98&v=1&r=http%3a%2f%2finnomet.ttu.ee%2fdaaam%2fproceedings%2fDesign%2520and%2520Production%2fStekleins.pdf&p=DevEx,5064.1

25. Stekleins, A., Gerins, E., Kromanis, A. Prediction of SiO2 Nano Coating Properties Using Fuzzy Logic. *DAAAM Proceedings Proceedings of the 28th International DAAAM Symposium 2017*. 2017, pp. 0654–0660. Available from: doi: 10.2507/28th.daaam.proceedings.092.
26. Stekleins, A., Gerins, E., Kromanis, A. Vacuum Gauge Performance Verification System. *Proceedings of the 27th International DAAAM Symposium 2016 DAAAM Proceedings*. 2016, pp. 0607–0614. Available from: doi: 10.2507/27th.daaam.proceedings.089.
27. Stekleins, A., Gerins, E., Kromanis, A. Vacuum Gauge Verification Methodology for Vacuum Coating Deposition Processes. *DAAAM Proceedings Proceedings of the 28th International DAAAM Symposium 2017*. 2017, pp.0645–0653. Available from: doi: 10.2507/28th.daaam.proceedings.091.
28. Stoiber, M., Badisch, E., Lugmair, C., Mitterer, C. Low-friction TiN coatings deposited by PACVD. *Surface and Coatings Technology*. 2003, Vol. 163–164, pp. 451–456. Available from: doi: 10.1016/s0257-8972(02)00642-4.
29. The Institute of Measurement and Control. *Guide to the Measurement of Pressure and Vacuum* [online]. London, 1998 [viewed 5 December 2017]. Available from: http://www.bing.com/cr?IG=284B417840A84703B3DAFEF5F78F4574&CID=0E51EF1A806065EA1956E455816664FD&rd=1&h=uN2DeD3oOWspF_r9C9JB34jXQQqUAu370hOnTcPL25s&v=1&r=http%3a%2f%2fwww.npl.co.uk%2fupload%2fpdf%2fGuide_to_PV.pdf&p=DevEx,5068.1
30. Tompkins, H. G. *The fundamentals of vacuum technology*. New York: Education Committee, American Vacuum Society, 1997. 199 p.
31. Ueda, E., Hirogata, Y., Hino, T., Yamashina, T. Lower limit of pressure measurement using a spinning rotor gauge. *Vacuum*. 1993, Vol.44, No. 5–7, pp. 587–589. Available from: doi: 10.1016/0042-207x(93)90102-g.
32. Vergöhl, M., Rademacher, D., Pflug, A. Progress on optical coatings deposited with dual rotatable magnetrons in a sputter up system. *Surface and Coatings Technology*. 2014, Vol. 241, pp. 38–44. Available from: doi: 10.1016/j.surfcoat.2013.11.033.
33. Vesel, A., Mozetič, M. Characteristics of a magnetron cold cathode gauge. *Vacuum*. 2004, Vol. 73, No. 2, pp. 281–284. Available from: doi: 10.1016/j.vacuum.2003.12.008.
34. Vesel, A., Mozetic, M., Zumer, M., Nemanic, V., Zajec, B. Pressure/current characteristics of a magnetron cold cathode gauge. *Vacuum*. 2005, Vol. 78, No. 1, pp. 13–17. Available from: doi: 10.1016/j.vacuum.2004.12.008.
35. Wang, X., Liu, C., Zhang, Z., Liu, S., Luo, X. A micro-machined Pirani gauge for vacuum measurement of ultra-small sized vacuum packaging. *Sensors and Actuators A: Physical*. 2010, Vol. 161, No. 1–2, pp. 108–113. Available from: doi: 10.1016/j.sna.2010.04.034.
36. Yoshida, H., Arai, K., Akimichi, H., Hirata, M. Stability tests of ionization gauges using two-stage flow-dividing system. *Vacuum*. 2009, Vol. 84, No. 5, pp. 705–708. Available from: doi: 10.1016/j.vacuum.2009.09.011.

37. Zhou, Q., Wu, W., Liu, D., Li, K., Qiao, Q. Estimation of corrosion failure likelihood of oil and gas pipeline based on fuzzy logic approach. *Engineering Failure Analysis*. 2016, Vol. 70, pp. 48–55. Available from: doi: 10.1016/j.engfailanal.2016.07.014.
38. Заде, Л. Понятие лингвистической переменной и его применение к принятию приближенных решений. Москва: Мир, 1976. 165 с.
39. Леоненков, А.В. Нечеткое моделирование в среде MATLAB и fuzzyTECH. Санкт Петербург: БВХ-Петербург, 2005. 736 с.
40. Розанов, Л. Н. Вакуумная техника: Учеб. для вузов по спец. Вакуумная техника 2-е изд., перераб. и доп. Москва: ВЫСШ. шк. 1990. 320 с.
41. Agilent Technologies: TV-3KT Pumping System User Manual / Internets. – http://www.agilent.com/cs/library/usermanuals/public/TV-3KT%20Pumping%20System%20User%20Manual.pdf
42. Bereau International des Poids et Mesures: Evaluation of measurement data – An introduction to the "Guide to the expression of uncertainty in measurement" and related documents / Internets. - http://www.bipm.org/en/publications/guides/gum.html
43. FILMETRICS. Reflectance Calculator / Internets. - http://www.filmetrics.com/reflectance-calculator
44. INFICON: HPG400 ATM to High-Vacuum Gauge / Internets. – http://products.inficon.com/en-us/Product/Detail/HPG400?path=Products%2Fpg-wide-range-vacuum-gauges
45. INFICON: SKY CDG025D Capacitance Diaphragm Gauge / Internets. – http://products.inficon.com/en-us/Product/Detail/CDG025D-X3?path=Markets_Applications%2FMarkets
46. INFICON: BPG402-Sx ATM to Ultra-High Vacuum Gauge / Internets. – http://products.inficon.com/en-us/Product/Detail/BPG402-S?path=Products%2Fpg-wide-range-vacuum-gauges
47. Latvijas Universitāte: Laboratorijas darbi studentiem / Internets. – http://www.cfi.lu.lv/fileadmin/user_upload/lu_portal/projekti/cfi/Studentiem/laboratorijas_darbi/Vakuumpaarklaajumu_LD_2010.pdf
48. LZA Terminoloģijas komisija: Akadēmiskā terminu datubāze AkadTerm / Internets. – http://termini.lza.lv/term.php?term=fazilo%C4%A3ika&list=&lang=LV
49. Rīgas Tehniskā Universitāte: Laboratorijas darbu apraksts (I semestris) un mērījumu rezultātu matemātiskās apstrādes pamati / Internets. – http://www.bf.rtu.lv/documents/nvsd/materiali/fizika/Laboratorijas%20darbu%20apraksts%20nekl.pdf
50. United Kingdom Accreditation Service: The Expression of Uncertainty and Confidence in Measurement JH 2012 / Internets. – https://www.ukas.com/download/publications/publications-relating-to-laboratory-accreditation/M3003_Ed3_final.pdf

APPENDICES

Appendix 1

Student's values depending on degrees of freedom

f	P = 0.90	P = 0.95	P = 0.98	P = 0.99
1	6.31	12.7	31.8	63.6
2	2.92	4.30	6.97	9.93
3	2.35	3.18	4.54	5.64
4	2.13	2.78	3.75	4.60
5	2.02	2.57	3.37	4.03
6	1.94	2.45	3.14	3.71
7	1.90	2.36	3.0	3.50
8	1.86	2.31	2.90	3.36
9	1.83	2.26	2.82	3.25
10	1.81	2.23	2.76	3.17
11	1.80	2.20	2.72	3.11
12	1.78	2.18	2.68	3.05

Appendix 2

Conversion table for units of throughput

	Pa m^3 / s = W	mbar l / s	Torr l / s	atm cm^3 / s	lusec	sccm	slm	Mol / s
Pa m^3 / s	1	10	7.5	9.87	$7.5 \cdot 10^3$	592	0.592	$4.41 \cdot 10^{-4}$
mbar l / s	0.1	1	0.75	0.987	750	59.2	$5.92 \cdot 10^{-2}$	$4.41 \cdot 10^{-5}$
Torr l / s	0.133	1.33	1	1.32	1,000	78.9	$7.89 \cdot 10^{-2}$	$5.85 \cdot 10^{-5}$
atm cm^3 / s	0.101	1.01	0.76	1	760	59.8	$5.98 \cdot 10^{-2}$	$4.45 \cdot 10^{-5}$
lusec	$1.33 \cdot 10^{-4}$	$1.33 \cdot 10^{-3}$	10-3	$1.32 \cdot 10^{-3}$	1	$7.89 \cdot 10^{-2}$	$7.89 \cdot 10^{-5}$	$5.86 \cdot 10^{-8}$
sccm	$1.69 \cdot 10^{-3}$	$1.69 \cdot 10^{-2}$	$1.27 \cdot 10^{-2}$	$1.67 \cdot 10^{-2}$	12.7	1	10-3	$7.45 \cdot 10^{-7}$
slm	1.69	16.9	12.7	16.7	$1.27 \cdot 10^4$	1,000	1	$7.45 \cdot 10^{-4}$
Mol / s	$2.27 \cdot 10^3$	$2.27 \cdot 10^4$	$1.7 \cdot 10^4$	$2.24 \cdot 10^4$	$1.7 \cdot 10^7$	$1.34 \cdot 10^6$	$1.34 \cdot 10^3$	1